

# Filamentation Regulatory Pathways Control Adhesion-Dependent Surface Responses in Yeast

Jacky Chow,\* Izzy Starr,\* Sheida Jamalzadeh,<sup>†</sup> Omar Muniz,<sup>\*,1</sup> Anuj Kumar,<sup>‡</sup> Omer Gokcumen,\*  
Denise M. Ferkey,\* and Paul J. Cullen<sup>\*,2</sup>

\*Department of Biological Sciences and <sup>†</sup>Department of Chemical and Biological Engineering, State University of New York at the University at Buffalo, New York 14260-1300 and <sup>‡</sup>Department of Molecular, Cell, and Developmental Biology, University of Michigan, Ann Arbor, Michigan 48109

ORCID IDs: 0000-0002-8923-297X (A.K.); 0000-0003-4371-679X (O.G.)

QA1

**ABSTRACT** Signaling pathways can regulate biological responses by the transcriptional regulation of target genes. In yeast, multiple signaling pathways control filamentous growth, a morphogenetic response that occurs in many species including fungal pathogens. Here, we examine the role of signaling pathways that control filamentous growth in regulating adhesion-dependent surface responses, including mat formation and colony patterning. Expression profiling and mutant phenotype analysis showed that the major pathways that regulate filamentous growth [fungal MAPK (fMAPK), RAS, retrograde (RTG), RIM101, RPD3, ELP, SNF1, and PHO85] also regulated mat formation and colony patterning. The chromatin remodeling complex, SAGA, also regulated these responses. We also show that the RAS and RTG pathways coregulated a common set of target genes, and that SAGA regulated target genes known to be controlled by the fMAPK, RAS, and RTG pathways. Analysis of surface growth-specific targets identified genes that respond to low oxygen, high temperature, and desiccation stresses. We also explore the question of why cells make adhesive contacts in colonies. Cell adhesion contacts mediated by the coregulated target, and adhesion molecule, Flo11p, deterred entry into colonies by macroscopic predators and impacted colony temperature regulation. The identification of new regulators (e.g., SAGA), and targets of surface growth, in yeast may provide insights into fungal pathogenesis in settings where surface growth and adhesion contributes to virulence.

**KEYWORDS** MAPK pathways; signaling networks; expression profiling; fungal pathogenesis; microbial predator–prey relationships; pseudohyphal growth; invasive growth; biofilm; mat; complex colony; temperature control

**F**UNGAL microorganisms exhibit a range of nutrient-related responses. Under certain conditions, fungal cells can differentiate into filamentous or hyphal cells that can expand across, and/or penetrate into, new environments (Soll and Daniels 2016). Many fungal species can also grow in communities of biofilms or mats, which are composed of interconnected cells that attach to each other and to surfaces. One property of mats is the formation of highly organized patterns that result from adhesive contacts between cells. In patho-

gens, filamentous growth (Lo *et al.* 1997) and biofilm formation (Desai *et al.* 2014) are critical determinants of virulence. For example, cells can adhere to medical devices and grow in dense mats that are resistant to antifungal medicines (Chandra *et al.* 2001; Sudbery *et al.* 2004; Kumamoto 2005; Ramage *et al.* 2005; Nett and Andes 2015).

The budding yeast *Saccharomyces cerevisiae* is a unicellular fungal microbe, and a convenient model for studying nutrient-regulated foraging responses like filamentous growth and mat formation. These responses are best studied in “wild” strain backgrounds (such as  $\Sigma$ 1278b) as the responses have been lost in certain laboratory strains due to genetic manipulation (Liu *et al.* 1996; Dowell *et al.* 2010; Chin *et al.* 2012). During filamentous growth, yeast cells differentiate into elongated and polarized filaments that remain connected in pseudohyphae (Gimeno *et al.* 1992; Cullen and Sprague 2012).

At least 600 genes have been identified by genetic screens (Lorenz and Heitman 1998; Palecek *et al.* 2000) and genome-wide

Copyright © 2019 by the Genetics Society of America

doi: <https://doi.org/10.1534/genetics.119.302004>

Manuscript received February 14, 2019; accepted for publication April 18, 2019; published Early Online May 3, 2019.

Available freely online through the author-supported open access option.

Supplemental material available at FigShare: <https://doi.org/10.25386/genetics.8066615>.

<sup>1</sup>Present address: University of Texas El Paso, TX 79968.

<sup>2</sup>Corresponding author: Department of Biological Sciences, State University of New York at the University at Buffalo, 341 Cooke Hall, Buffalo, NY 14260-1300. E-mail: [pcullen@buffalo.edu](mailto:pcullen@buffalo.edu)

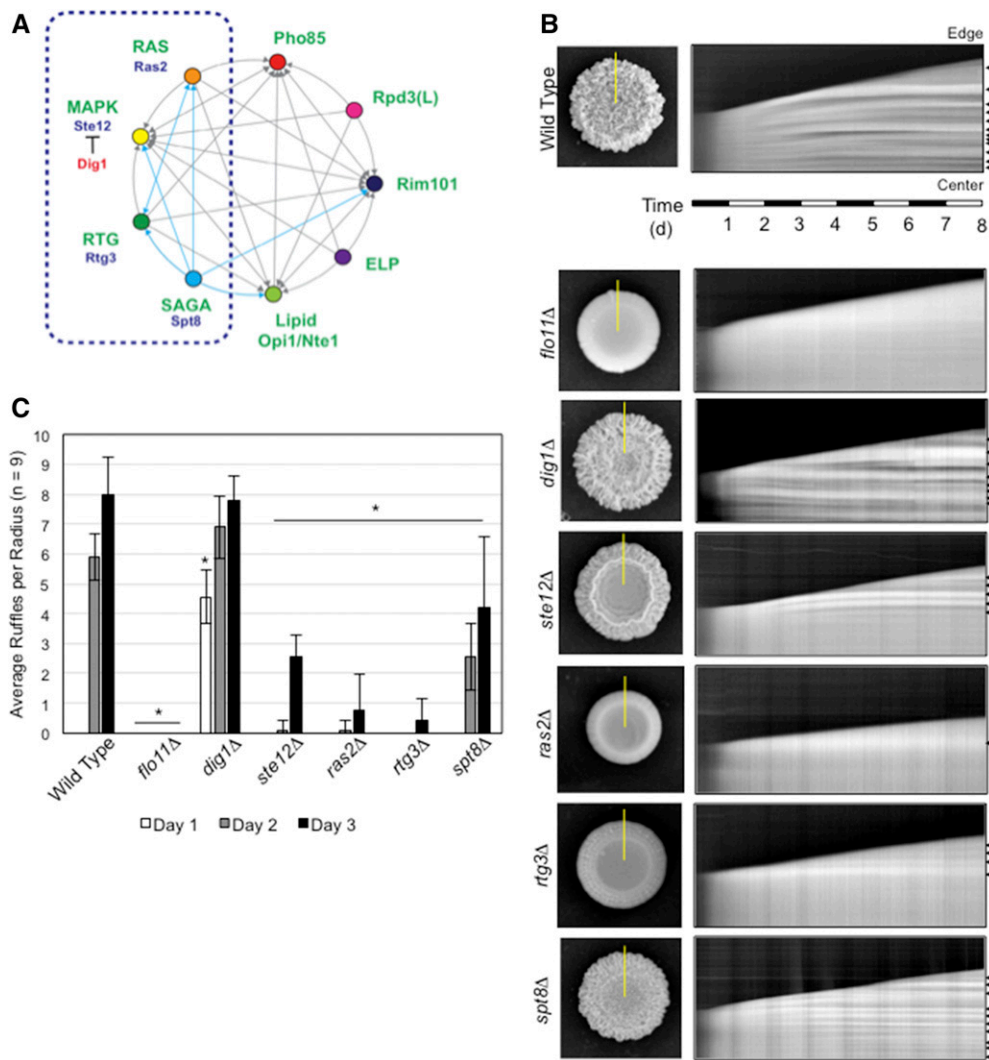


**Figure 1** Functionally interconnected signaling pathways regulate mat expansion and colony pattern formation over time. (A) Circles represent signaling pathways or regulatory complexes that control filamentous growth. Arrows refer to target genes coregulated by pathways, as adapted from Chavel *et al.* (2014). Cyan arrows refer to functional connections identified in this study. The dashed blue box marks the part of the network on which the study is focused. (B) Time-course experiment of colony pattern formation in wild-type cells and the indicated mutants. Colony expansion was examined over an 8-day time period (Videos S1–S7). In the left panels, colonies at the 8-day time period are shown. On the right are kymographs that show colony expansion over time. The yellow lines in the left panels refer to the region selected for kymograph analysis. The panels on the right show colony patterns that developed over time in the region selected by the yellow line, where the bottom of the figure represents the colony center and the top represents the colony perimeter (edge). Arrows mark features that are characteristic of ruffle formation, which is quantitated in (C). (C) Bar graph showing the average number of ruffles in wild-type and the indicated mutant colonies at  $t = 1$  day (white), 2 days (gray), and 3 days (black). Error bars represent SD among nine radii from three biological replicates. \*  $P < 0.05$  between the mutant and wild-type for the same time point.

studies (Jin *et al.* 2008; Xu *et al.* 2010; Ryan *et al.* 2012) that play some role in filamentous growth. A subset of these genes encode signaling pathway components that include at least four major nutrient-sensing pathways [fungal MAPK (fMAPK), RAS, TOR (target of rapamycin), and SNF1], as well as pathways that regulate the response to pH (RIM101), phosphate utilization (PHO85), and mitochondrial stress [the retrograde mitochondria-to-nucleus (RTG) pathway]. In addition, proteins that control the epigenetic modification of histones to alter gene expression have also been implicated in the regulation of filamentous growth (Rpd3p).

Many of the pathways that regulate filamentous growth are functionally connected through their ability to coregulate common target genes (Figure 1A). In some cases, this occurs at the level of transcription. In a pioneering study, it was shown that many of the transcription factors that control filamentous growth control each other's expression (Borneman *et al.* 2006). Transcription factors can also converge at common promoter elements. One example is the

gene encoding the major cell adhesion molecule in yeast, Flo11p (Kraushaar *et al.* 2015; Chan *et al.* 2016). The *FLO11* gene contains one of the largest and most highly regulated promoters in the yeast genome, and functions as a “hub” where multiple transcription factors and chromatin remodeling enzymes bind (Robertson and Fink 1998; Rupp *et al.* 1999; Palecek *et al.* 2000; Pan and Heitman 2000; Kuchin *et al.* 2002; van Dyk *et al.* 2005; Barrales *et al.* 2008). Signaling pathways that control filamentous growth can also regulate each other's activity. The classic example comes from the discovery that the RAS pathway can regulate the activity of the fMAPK pathway (Mösch *et al.* 1996). It is now clear that many pathways regulate the activity of the fMAPK pathway (Chavel *et al.* 2010, 2014). One way this may occur is through the protein kinases of the major regulatory pathways, which can regulate each other's localization and activity (Bharucha *et al.* 2008).

187 Yeast can also undergo mat formation (Reynolds and Fink  
188 2001; Bojsen *et al.* 2012), where colonies expand radially  
189 across surfaces and form ruffled patterns (Granek and Mag-  
190 wene 2010; Granek *et al.* 2011; Tam *et al.* 2018). Mats form  
191 wheel-spoke patterns in low-percentage agar media [0.3%  
192 agar (Reynolds and Fink 2001)], and wrinkled or ruffled  
193 colonies on high-percentage agar media [1–4% (Granek  
194 and Magwene 2010; Karunanithi *et al.* 2012)]. Mat expan-  
195 sion and patterning require contacts between cells that are  
196 also mediated by Flo11p. Regulators of mat formation have  
197 been identified by direct approaches (Reynolds 2006; Sarode  
198 *et al.* 2011; Váchová *et al.* 2011), genome-wide deletion  
199 screens (Ryan *et al.* 2012; Voordeckers *et al.* 2012; Scherz  
200 *et al.* 2014), overexpression screens (Cromie *et al.* 2017), and  
201 comparative expression profiling (Traven *et al.* 2012;  
202 Maršíková *et al.* 2017). Many of the molecular pathways that  
203 control mat formation regulate FLO11 expression. In addi-  
204 tion, several regulators of mat formation, like the cell wall  
205 integrity sensor Wsc1p (Sarode *et al.* 2014) and vacuolar  
206 protein-sorting genes (Sarode *et al.* 2011), appear to regulate  
207 mat formation by mechanisms that do not involve Flo11p.  
208 Despite the identification of many proteins and pathways  
209 that regulate mat formation, the benefits that cells derive  
210 from forming these complex patterns remain unclear. Fur-  
211 thermore, the stresses encountered during colonial surface  
212 growth remain relatively unexplored.

213 As seen in other fungi, filamentous growth and mat for-  
214 mation are related responses in yeast. Both responses require  
215 Flo11p (Lo and Dranginis 1998; Reynolds and Fink 2001),  
216 and a corresponding set of regulatory proteins and pathways  
217 that control FLO11 expression (Ryan *et al.* 2012). These in-  
218 clude the TOR (Cutler *et al.* 2001; Bojsen *et al.* 2016),  
219 Rim101 (Li and Mitchell 1997; Sarode *et al.* 2011;  
220 Voordeckers *et al.* 2012), fMAPK (Roberts and Fink 1994;  
221 Reynolds and Fink 2001; Granek and Magwene 2010), and  
222 RAS pathways (Gimeno *et al.* 1992; Granek and Magwene  
223 2010; Zara *et al.* 2011; Ryan *et al.* 2012; Bojsen *et al.* 2016).  
224 The tRNA modification complex elongator (ELP) regulates all  
225 three responses (Abdullah and Cullen 2009). It has also been  
226 shown that under nutrient-limiting conditions, mats are com-  
227 posed of filamentous cells (Karunanithi *et al.* 2012). Given  
228 the abovementioned connections between filamentous  
229 growth and mat formation, we sought to further define  
230 how the network of signaling pathways that control filamen-  
231 tous growth might regulate adhesion-dependent surface  
232 growth.

233 To learn more about the regulation of surface growth in  
234 yeast, adhesion-dependent surface responses were examined  
235 from several perspectives. In one set of experiments, we de-  
236 veloped a method for recording colony pattern formation over  
237 time by kymograph analysis, which allowed us to confirm that  
238 the major signaling pathways that control filamentous growth  
239 also regulate mat formation. A new regulator of filamentous  
240 growth, the chromatin remodeling complex SAGA, was also  
241 uncovered. Comparative expression profiling identified a  
242 large number of target genes as well as new regulatory

connections between pathways. By seeking to understand  
why cells form adhesive connections during surface growth,  
we identified a role for Flo11p in protection from macroscopic  
predators. We also showed that colony ruffling aids in tem-  
perature regulation. Our findings broaden the role of fila-  
mentation regulatory pathways to include the regulation of  
adhesion-dependent surface responses. Our findings may be  
relevant to studies of fungal pathogens that must tolerate  
growth on surfaces to become virulent.

## Materials and Methods

### Media and growth conditions

Yeast strains were grown and manipulated by standard meth-  
ods (Sambrook *et al.* 1989; Rose *et al.* 1990). For most ex-  
periments, colonies were grown on standard YPD (2%) or  
YEP-galactose (Gal) semisolid agar media (Cullen 2015a).  
Some experiments were performed on low-agar (0.3%) me-  
dia. Glutamate sensitivity experiments used synthetic agar  
(dextrose, 2%; yeast nitrogen base, 6.7 g/liter; uracil,  
20 mg/liter; His, 20 mg/liter; Leu, 120 mg/liter; adenine,  
20 mg/liter; Lys, 60 mg/liter; Arg, 20 mg/liter; Trp,  
20 mg/liter; Tyr, 30 mg/liter; Thr, 200 mg/liter; Met,  
20 mg/liter; and Phe, 50 mg/liter), minimal agar (dextrose,  
2%; yeast nitrogen base, 6.7 g/liter; and uracil, 20 mg/liter),  
and minimal + Glu (dextrose, 2%; yeast nitrogen base, 6.7 g/  
liter; uracil, 20 mg/liter; and Glu 20 mg/liter) media. To  
generate low-oxygen (5–15% oxygen) and anaerobic condi-  
tions, agar plates were incubated in GasPAK EZ Campy Pouch  
System (BD 260685; Becton, Dickinson and Company, Frank-  
lin Lakes, NJ) or BD GasPAK EZ Anaerobe Pouch System (BD  
260683; Becton, Dickinson and Company) bags. To maintain  
consistent moisture levels, plates were poured and left  
unwrapped for 3 days at 22° to allow the evaporation of  
excess moisture. To generate media with reduced moisture  
levels, YPD plates were left unwrapped for 10 days at 22°.

### Strains and genetic manipulations

Yeast strains are listed in Table 1. Gene deletions were con-  
structed using auxotrophic markers amplified by PCR and  
introduced into yeast by lithium acetate transformation by  
standard methods as described (Gietz and Schiest 2007). To  
generate the *spt8Δ* mutant, homologous recombination at  
the SPT8 locus was performed using the pKIURA3  
(PC5225) cassette as a template. For some experiments,  
yeast strains were used from an ordered knockout collection  
(Ryan *et al.* 2012). *Caenorhabditis elegans* strains used in this  
study include N2 Bristol wild-type and KP4 *glr-1(n2461)*  
(Kaplan and Horvitz 1993). Strains were maintained at 20°  
under standard conditions on nematode growth media  
(NGM) agar plates seeded with OP50 *Escherichia coli* bacteria  
(Brenner 1974).

**Table 1 Yeast strains used in the study**

Strain <sup>a</sup>	Description	Reference
PJ69-4A <sup>b</sup>	<i>MATa trp1-901 leu2-3,112 ura3-52 his3-200 ga14Δ ga180Δ LYS2::GALI-HIS3 GAL2-ADE2 met2::GAL7-lacZ</i>	James et al. (1996)
PC313	<i>MATa ura3-52</i>	Liu et al. (1993)
PC538	<i>MATa ura3-52 ste4 FUS1-lacZ FUS1-HIS3</i>	Cullen et al. (2004)
PC549	<i>MATa ura3-52 ste4 FUS1-lacZ FUS1-HIS3 ste20::URA3</i>	Cullen and Sprague (2000)
PC555	<i>MATa ura3-52 ste4 FUS1-lacZ FUS1-HIS3 hsl7::URA3</i>	Cullen and Sprague (2000)
PC562	<i>MATa ura3-52 ste4 FUS1-lacZ FUS1-HIS3 ras2::URA3</i>	Cullen and Sprague (2002)
PC611	<i>MATa ura3-52 ste4 FUS1-lacZ FUS1-HIS3 ste11::URA3</i>	Cullen and Sprague (2002)
PC999	<i>MATa ura3-52 ste4 FUS1-lacZ FUS1-HIS3 MSB2-HA</i>	Chavel et al. (2010)
PC1029	<i>MATa ura3-52 ste4 FUS1-lacZ FUS1-HIS3 flo11::KanMX6</i>	Karunanithi et al. (2010)
PC1079	<i>MATa ura3-52 ste4 FUS1-lacZ FUS1-HIS3 ste12::URA3</i>	Karunanithi et al. (2010)
PC2523	<i>MATa ura3-52 ste4 FUS1-lacZ -::NAT FUS1-HIS3 flo8::HYG</i>	Chavel et al. (2010)
PC2712	<i>MATa ura3-52 ste4 FUS1-lacZ FUS1-HIS3 GAL-FLO11::KanMX6</i>	Karunanithi et al. (2010)
PC3030	<i>MATa ura3-52 ste4 FUS1-lacZ FUS1-HIS3 MSB2-HA sin3::NAT</i>	Chavel et al. (2010)
PC3039	<i>MATa ura3-52 ste4 FUS1-lacZ FUS1-HIS3 MSB2-HA dig1::NAT</i>	Chavel et al. (2010)
PC3431	<i>MATa ura3-52 ste4 FUS1-lacZ -::NAT FUS1-HIS3 MSB2-HA sfl1::KIURA3</i>	Chavel et al. (2010)
PC3642	<i>MATa ste4 FUS1-lacZ FUS1-HIS3 ura3-52 MSB2-HA rtg3::NAT</i>	Chavel et al. (2010)
PC3652	<i>MATa ste4 FUS1-lacZ FUS1-HIS3 ura3-52 MSB2-HA rtg2::NAT</i>	Chavel et al. (2010)
PC3695	<i>MATa ste4 FUS1-lacZ FUS1-HIS3 ura3-52 MSB2-HA rtg1::NAT</i>	Chavel et al. (2014)
PC4005	<i>MATa ste4 FUS1-lacZ FUS1-HIS3 ura3-52 gcn5::KIURA3</i>	This study
PC3688	<i>MATa ste4 FUS1-lacZ FUS1-HIS3 ura3-52 opi1::NAT</i>	Chavel et al. (2010)
PC4008	<i>MATa ura3-52 ste4 FUS1-lacZ FUS1-HIS3 spt8::KIURA3</i>	This study
PC5090	<i>MATa ura3-52 ste4 FUS1-lacZ FUS1-HIS3 nte1::NAT</i>	Chavel et al. (2014)
PC5119	<i>MATa ura3-52 ste4 FUS1-lacZ FUS1-HIS3 pho80::NAT</i>	This study
PC6733	<i>MATa ura3-52 ste4 FUS1-lacZ FUS1-HIS3 ura3-52::pTEF2-mCherry URA3 his5::NAT mCherry::GFPy-HIS</i>	Chow et al. (2019)
PC6016	<i>MATa can1Δ::Ste2pr-spHIS5 lyp1Δ::Ste3pr-LEU2 his3::hisG leu2Δ0 ura3Δ0</i>	Ryan et al. (2012)
CB13A9 <sup>c</sup>	<i>MATa can1Δ::Ste2pr-spHIS5 lyp1Δ::Ste3pr-LEU2 his3::hisG leu2Δ0 ura3Δ0 dan1Δ</i>	Ryan et al. (2012)
CB52G2	<i>MATa can1Δ::Ste2pr-spHIS5 lyp1Δ::Ste3pr-LEU2 his3::hisG leu2Δ0 ura3Δ0 sip18Δ</i>	Ryan et al. (2012)
CB53F12	<i>MATa can1Δ::Ste2pr-spHIS5 lyp1Δ::Ste3pr-LEU2 his3::hisG leu2Δ0 ura3Δ0 sno4Δ</i>	Ryan et al. (2012)
CB60E1	<i>MATa can1Δ::Ste2pr-spHIS5 lyp1Δ::Ste3pr-LEU2 his3::hisG leu2Δ0 ura3Δ0 gre1Δ</i>	Ryan et al. (2012)
CB29E8	<i>MATa can1Δ::Ste2pr-spHIS5 lyp1Δ::Ste3pr-LEU2 his3::hisG leu2Δ0 ura3Δ0 hsp26Δ</i>	Ryan et al. (2012)

<sup>a</sup> Unless indicated, strains are derived from the Σ1278b strain background.

<sup>b</sup> Strain from M. Johnston's laboratory.

<sup>c</sup> Strains from an ordered deletion collection labeled with "CB" followed by the plate number and location.

### Assays for mat formation and filamentous growth

Assays for mat formation were performed as described (Reynolds and Fink 2001; Karunanithi et al. 2012). The plate-washing assay was performed as described (Cullen 2015b).

### Microscopy

Mats were examined by bright-field microscopy using an Axioplan 2 fluorescent microscope (Zeiss [Carl Zeiss], Thornwood, NY) with 5×, 10×, 20×, 40×, and 100× PLAN-APOCHROMAT 100×/1.4 (oil) (N.A. 0.17) objectives. Digital images were obtained with an Axiocam MRm camera (Zeiss). Axiovision 4.4 software (Zeiss) was used for image acquisition. Digital images were imported into ImageJ (<https://imagej.nih.gov/ij/>) in 8-bit format.

### Comparative RNA sequencing analysis

To compare the transcriptional response of wild-type cells (PC538) and the *ste12Δ* (PC1079), *dig1Δ* (PC3039), *rtg3Δ* (PC3642), *spt8Δ* (PC4008), and *ras2Δ* (PC562) mutants, cells were concentrated (OD<sub>A600</sub> = 20) and spotted in 10-μl aliquots onto YEP-Gal (2% agar) for 24 hr. Cells were spotted as six colonies per plate, equidistant to each other and the plate center. All six colonies were harvested for each trial and three separate trials were compared for each strain. The entire colony surface was scraped into 500 μl of distilled water, harvested by centrifugation, washed, and stored at -80°. RNA was harvested by hot-acid phenol-chloroform extraction as described (Adhikari and Cullen 2014). Samples were further purified using a QIAGEN RNeasy Mini Kit (catalog number 74104; QIAGEN, Valencia, CA). RNA concentration and purity was measured via NanoDrop (NanoDrop

2000C; Thermo Fisher Scientific, Waltham, MA). RNA stability was determined by running the sample on an agarose gel.

RNA sequencing (RNA-seq) was performed as described previously (Adhikari and Cullen 2014) by sequencing RNA prepared from three separate cultures. RNA-seq libraries were prepared from total RNA using the TruSeq RNA Sample Prep Kit (Illumina, San Diego, CA). Library size distributions were validated using an Agilent 2200 TapeStation (Agilent Technologies, Santa Clara, CA). Additional library quality control, blending of pooled indexed libraries, and cluster optimization was performed using Invitrogen's Qubit 2.0 Fluorometer (Invitrogen, Carlsbad, CA). RNA-seq libraries were pooled (21-plex) and clustered onto a flow cell lane using an Illumina cBot. Sequencing was performed using an Illumina HiSeq 2500 in Rapid Mode employing a paired-end, 50-base read length (PE50) sequencing strategy.

Image analysis and base calling were performed using Illumina's Real Time Analysis v1.18 software, followed by "demultiplexing" of indexed reads and generation of FASTQ files, using Illumina's bcl2fastq Conversion Software v1.8.2 ([http://support.illumina.com/downloads/bcl2fastq\\_conversion\\_software\\_184.html](http://support.illumina.com/downloads/bcl2fastq_conversion_software_184.html)). For analysis of the RNA-seq data, reads of low quality were filtered out prior to alignment to the reference genome (*S. cerevisiae* assembly R64-1-1, Ensembl release 75) using TopHat v2.0.9 (Trapnell *et al.* 2009). Counts were generated from TopHat alignments for each gene using the Python package HTSeq v0.6.1 (Anders *et al.* 2015). Genes with low counts across all samples were removed.

For comparisons of mutant to wild-type colony samples, differentially expressed genes were identified using the Bioconductor package DESeq2 (Love *et al.* 2014) with the apeglm package to estimate t-prior shrinkage (Zhu *et al.* 2018). We employed the IHW package to weight hypotheses and optimize power (Ignatiadis *et al.* 2016). Differential expression was defined as  $|\log_2(\text{ratio})| \geq 0.585$  ( $\pm 1.5$  fold) with  $P < 0.01$ . Genes were categorized as "upregulated" ( $\log_2(\text{fold change}) > 0.585$ ,  $P\text{-value} < 0.01$ ), "down-regulated" ( $\log_2(\text{fold change}) < -0.585$ ,  $P\text{-value} < 0.01$ ), or "insignificant" ( $\log_2(\text{fold change}) < -0.585$  or  $\log_2(\text{fold change}) > 0.585$ ,  $P\text{-value} > 0.01$ ). Differentially expressed pathway-specific genes were visualized in principal component analysis (PCA), volcano plot, and Venn diagram figures using ggplot2. Pathway-specific gene expression was visualized using the Kyoto Encyclopedia of Genes and Genomes (Kanehisa and Goto 2000), and the Bioconductor package pathview (Luo and Brouwer 2013). Classification of targets was based on gene ontology (GO) terms and descriptions in the *Saccharomyces* Genome Database (<http://www.yeastgenome.org>). For all other comparisons, edgeR v3.18.1 (Robinson *et al.* 2010) was used. A false discovery rate (FDR) method was employed to correct for multiple testing (Reiner *et al.* 2003). Differential expression was defined as  $|\log_2(\text{ratio})| \geq 0.585$  ( $\pm 1.5$  fold) with  $P\text{-value} < 0.01$ .

## GO term analysis

GO term analysis (Ashburner *et al.* 2000) was performed using the GO enrichment analysis and visualization tool (GORilla) (Eden *et al.* 2007, 2009) using the two unranked lists mode. The Gorilla database had been last updated January 12, 2019. The background list was all of the ORFs identified during the analysis. The target list for genes regulated by all five regulators was identified as genes whose  $|\log_2\text{FC}| > 0.585$  and  $P\text{-value} < 0.01$  in all mutant sets. The target list for genes regulated by both RAS and RTG was identified as genes  $|\log_2\text{FC}| > 0.585$  and  $P\text{-value} < 0.01$  in only the *ras2* $\Delta$  and *rtg3* $\Delta$  sets. Enriched GO terms were identified by having  $P < 10^{-3}$  and  $\text{FDR} < 0.05$ . Values for background and target sets, and enriched GO terms, are in Supplemental Material, Table S2.

## Quantitative PCR analysis

Differential gene expression was confirmed by quantitative (q) real-time PCR analysis as described previously (Chavel *et al.* 2014). cDNA libraries from RNA samples were generated using iScript Reverse Transcriptase Supermix (catalog number 1708840; Bio-Rad, Hercules, CA). qPCR was performed using iTaq Universal SYBR Green Supermix (catalog number 1725120; Bio-Rad) on the Bio-Rad CFX384 Real-Time System. Primers were ordered from Sigma ([Sigma Chemical], St. Louis, MO) and are listed in Table S3. FCs in expression were determined by calculating  $\Delta\Delta\text{Ct}$  (Livak and Schmittgen 2001) using *ACT1* mRNA as the housekeeping gene for each sample. RNA was prepared from at least three samples and the average of at least three biological replicates was recorded. Statistical significance was determined by the Student's *t*-test.

## Time-lapse photography

Cells were grown on YEP-Gal semisolid agar media at 22° for 8 days. Photographs were taken using a Nikon D3000 (Nikon, Garden City, NY) digital camera at 30-min intervals using automatic exposure without flash. Graph paper (0.25 cm) was glued to the plate bottom for scaling and later image stabilization; these were cropped out in the final images. Images were imported into ImageJ as an image stack for image stabilization using Kang Li's image stabilizer plug-in ([http://www.cs.cmu.edu/~kangli/code/Image\\_Stabilizer.html](http://www.cs.cmu.edu/~kangli/code/Image_Stabilizer.html)). Stabilized image series were saved in video format. Kymographs were generated using the reslice tool in ImageJ (<https://imagej.nih.gov/ij/>).

Ruffles were identified as light bands flanked by dark bands. The number of ruffles per time point was counted manually at 1-day intervals for each kymograph. Statistical analysis was carried out for each time point using an unpaired Student's *t*-test.

## Evaluation of phosphorylated Kss1 levels

Samples were harvested at specific distances from the colony perimeter at  $t = 0$ . To determine P-Kss1p levels at the

growing edge of a colony, the outermost millimeters of representative colonies were harvested at 1, 2, 3, and 4 days. To determine the changes in P-Kss1p levels before and after the colony ruffles, samples were harvested from regions of the colony 2 mm from the starting colony edge from representative colonies before and after ruffling.

Samples were evaluated by SDS-PAGE analysis. Immunoblots were performed as described (Cullen 2015a). P-Kss1p was detected with phospho-p44/42 primary antibodies (catalog number 4370S; Cell Signaling Technology, Danvers, MA) and anti-rabbit HRP secondary antibodies (catalog number 111-035-144; Jackson ImmunoResearch, West Grove, PA). Total Kss1p was detected by anti-Kss1p antibodies (SC-6775-R; Santa Cruz Biotechnology, Dallas, TX) and with anti-rabbit HRP secondary antibodies (catalog number 111-035-144; Jackson ImmunoResearch). Loading control Pgk1p was identified by anti-Pgk1p primary antibodies (catalog number 459250; Invitrogen) and with anti-mouse HRP secondary antibodies (catalog number 1706516; Bio-Rad).

### **Effect of *S. cerevisiae* cell-cell adhesion on pharyngeal uptake by *C. elegans***

Wild-type yeast cells expressing GFP (PC6733) were grown in synthetic or YPD liquid media at 30° for 16 hr. Cells were washed twice in M9 buffer (KH<sub>2</sub>PO<sub>4</sub>, 3 g/liter; Na<sub>2</sub>HPO<sub>4</sub>, 6 g/liter; NaCl, 5 g/liter; and 1 mM MgSO<sub>4</sub>). As previously described (Bois *et al.* 2013), adult *C. elegans* were transferred into suspensions of *S. cerevisiae*. After 45 min, *C. elegans* were removed and mounted onto 2% agarose pads, and immobilized with 10 mM sodium azide. Slides were examined with an Axioplan 2 fluorescent microscope (Zeiss) at 40×. Individual *S. cerevisiae* cells were counted. Independent replicates were performed on three separate days.

### **Experiments involving yeast colonies exposed to entry by *C. elegans***

Yeast cells were grown in YPD liquid media at 30° for 16 hr. For interactions between *C. elegans* and *S. cerevisiae* colonies, 200-μl aliquots of cells were dispensed onto NGM (Wood 1988) agar media and grown as colonies at 22° for 72 hr. Under this condition, yeast colonies formed Flo11p-dependent patterns. OP50 *E. coli* (Brenner 1974) were taken from stock cultures, and 200 μl aliquots were dispensed onto NGM agar media and grown at 22° for 3 days.

To examine colony penetration, adult and fourth-stage larva (L4) *C. elegans* were transferred from stock OP50 plates to experimental plates around the yeast or *E. coli*. Mat penetration times were determined by measuring the time from a worm nose first contacting the colony to the tail fully entering the mat, up to 100 sec. The number of stalls and reversals was determined by counting the number of incidents when a worm's tail would stop forward movement or reverse. The percent of time moving forward was determined by recording the amount of time that a worm was moving forward divided by the total time required to penetrate a mat. Independent replicates were performed on at least three separate days.

To examine the pharyngeal uptake of *S. cerevisiae* by *C. elegans*, wild-type (PC538) and *flo11Δ* (PC1029) yeast were transformed with a plasmid containing GFP-2xPH (PC2560) [CS189 (Stefan *et al.* 2005) provided by the Emr laboratory (Cornell University)]. Cells were grown in YPD liquid media at 30° for 16 hr and 200-μl aliquots were spotted onto NGM agar media. Colonies were grown at 22° for 3 days. Worms were transferred directly into colonies and left for 45 min before mounting and imaging. Independent replicates were performed on three separate days.

Video was captured using an AmScope MD35 camera and AmScope image capture software. The camera was inserted into the eyepiece of a Zeiss SteREO Discovery V8. Dot plots for worm entry times were generated in ggplot2 (Wickham 2016). Statistical analysis was performed using the Student's *t*-test.

### **Infrared imaging**

Infrared images were taken using FLIR A325sc (FLIR Systems, Wilsonville, OR) and captured using FLIR ResearchIRMax4 (FLIR Systems), provided by the Sustainable Manufacturing And Robotic Technology center at the University at Buffalo. Average and coolest temperatures for each colony were measured using FLIR ResearchIRMax4 (FLIR Systems).

An insulated housing unit was built to mount the thermal imaging camera above a stage for agar plates. Yeast cells were grown in YPD liquid media at 30° for 16 hr. Next, 10-μl aliquots were spotted onto YEP-Gal agar media. Colonies were grown for 72 hr at 30°. For imaging, plates were transferred from the incubator to the mount in a photographing area with an ambient temperature of 22°. Plate lids were removed to allow imaging. Images were taken immediately after removing the lid.

### **Data availability**

All strains are available upon request. The Gene Expression Omnibus (GEO) accession number for raw sequencing data is GSE115657. A comparison with previously published expression profiling data sets for cells grown in liquid culture has been described [GEO accession number GSE61783 (Adhikari and Cullen 2014)]. Supplemental material available at FigShare: <https://doi.org/10.25386/genetics.8066615>.

## **Results**

### **A signaling network regulates adhesion-dependent surface responses in yeast**

Multiple signal transduction pathways regulate filamentous growth (Figure 1A) (Chavel *et al.* 2010, 2014). A large number of genes that control invasive growth, pseudohyphal formation, and mat formation show significant overlap based on a genome-wide analysis using deletion mutants in the filamentous strain background (Ryan *et al.* 2012). Thus, we examined and compared how the signaling network that regulates filamentous growth impacts adhesion-dependent

635 surface responses in yeast. We sought to directly compare key  
636 pathways in the network (MAPK and RAS) to less well-char-  
637 acterized pathways (RTG) and to a newly identified chroma-  
638 tin remodeling complex (SAGA). All of the pathways were  
639 studied in reference to a key target adhesion molecule,  
640 Flo11p.


641 Some strains (e.g.,  $\Sigma$ 1278b) exhibit ruffled colony mor-  
642 phology when grown on surfaces. This phenotype is depen-  
643 dent on cell adhesion contacts mediated by Flo11p (Reynolds  
644 and Fink 2001; Karunanithi *et al.* 2012). To evaluate colony  
645 pattern formation, we performed a time-course experiment  
646 followed by kymograph analysis, which can reveal changes in  
647 local features over time (Kaksonen *et al.* 2003). Wild-type  
648 cells were spotted on 2% agar media (YEP-Gal), and ruffle  
649 formation was examined by photographing colonies at  
650 30-min intervals over an 8-day period (Video S1). In a series  
651 of experiments, kymographs were generated along multiple  
652 radii of expanding colonies to measure the extent of ruffle  
653 formation [Figure 1B, wild-type (PC538), yellow line corre-  
654 sponds to one kymograph at right]. Ruffles were identified as  
655 light horizontal bands flanked by dark bands and could be  
656 counted manually by this method (Figure 1B, wild-type,  
657 black arrows). Measuring the banding pattern from separate  
658 sections of the colony allowed us to assess the extent of ruffle  
659 formation over time (Figure 1C, wild-type). As has been pre-  
660 viously demonstrated (Granek and Magwene 2010), colonies  
661 lacking the adhesion molecule Flo11p did not form ruffles  
662 (Video S2), which was also evident by kymograph analysis  
663 [Figure 1, B and C and Figure S1, *flo11 $\Delta$*  (PC1029)]. There-  
664 fore, kymograph analysis permitted the numerical assess-  
665 ment of pattern formation in yeast colonies. In principle,  
666 kymograph analysis may allow quantification of colony pat-  
667 tern formation in other microbial systems.

668 Kymograph analysis was next applied to mutants lacking  
669 key components of the major signaling pathways that regulate  
670 filamentous growth. As expected (Roberts and Fink 1994;  
671 Rupp *et al.* 1999; Reynolds and Fink 2001; Granek and Mag-  
672 wene 2010), the fMAPK pathway was required for colony  
673 ruffling. Specifically, kymograph analysis showed that col-  
674 onies lacking a negative regulator of the fMAPK pathway,  
675 Dig1p (Cook *et al.* 1996; Tedford *et al.* 1997; Bardwell  
676 *et al.* 1998; Olson *et al.* 2000; Breikreutz *et al.* 2003;  
677 Kusari *et al.* 2004; Chou *et al.* 2006; van der Felden *et al.*  
678 2014), formed more ruffles than wild-type after 1 day of  
679 growth [Figure 1, B and C, *dig1 $\Delta$*  (PC3039), Figure S1, and  
680 Video S3], though this difference was less apparent over  
681 longer time periods. Conversely, loss of the fMAPK transcrip-  
682 tion factor, Ste12p, led to a defect in colony ruffling at the  
683 examined time points [Figure 1, B and C, *ste12 $\Delta$*  (PC1079),  
684 Figure S1, and Video S4]. The fMAPK pathway was also re-  
685 quired for mat formation on 0.3% agar (Figure S1; *ste12 $\Delta$*   
686 and *dig1 $\Delta$* ; Figure S2 provides examples of other fMAPK reg-  
687 ulators; *ste11 $\Delta$*  and *ste20 $\Delta$* ). Also as expected (Gimeno *et al.*  
688 1992; Rupp *et al.* 1999; Granek and Magwene 2010; Zara  
689 *et al.* 2011; Ryan *et al.* 2012), the RAS pathway was required  
690 for colony ruffling [Figure 1, B and C, *ras2 $\Delta$*  (PC562) and

691 Video S5] and mat formation (Figures S1 and S2). Thus,  
692 kymograph analysis can be used to evaluate the roles of sig-  
693 naling pathways in regulating aspects of mat and colony pat-  
694 tern formation.

695 We next tested whether other pathways that are known to  
696 regulate filamentous growth also regulated adhesion-depen-  
697 dent colonial responses. The mitochondria-to-nucleus RTG  
698 pathway regulates invasive growth (Chavel *et al.* 2010;  
699 González *et al.* 2017). We also found that the RTG pathway  
700 was also required for colony ruffling [Figure 1, B and C, *rtg3 $\Delta$*   
701 (PC3642), Figure S3, and Video S6] and mat formation on  
702 0.3% agar (Figures S1 and S2).

703 We next tested the role of other proteins that control  
704 filamentous growth. Pho85p regulates filamentous growth  
705 (Chavel *et al.* 2010) and was also required for mat formation  
706 (Figure S1 and S2). Rpd3p (Chavel *et al.* 2010; Voordeckers  
707 *et al.* 2012), lipid regulators Opi1p and Nte1p (Chavel *et al.*  
708 2014), and Snf1p (Cullen and Sprague 2000; Voordeckers  
709 *et al.* 2012) were also required for mat formation (Figures S1  
710 and S2). Based on these results, we conclude that many of the  
711 major signaling pathways that regulate filamentous growth  
712 also regulate mat formation and colony patterning.


713 We hypothesized that the chromatin remodeling complex  
714 SAGA (Koutelou *et al.* 2010) might also regulate adhesion-  
715 dependent surface growth. The hypothesis was based on the  
716 fact that a component of SAGA, Gcn5p (Georgakopoulos and  
717 Thireos 1992; Sterner and Berger 2000), is required for fila-  
718 mentous growth (Chavel *et al.* 2014). Moreover, SAGA com-  
719 ponents have previously been shown to control aspects of  
720 colonial patterning (Voordeckers *et al.* 2012). Spt8p, a SAGA  
721 component (Winston *et al.* 1987), also regulates filamentous  
722 growth (Voordeckers *et al.*, personal communication). Kymograph  analysis of the *spt8 $\Delta$*   
723 mutant showed a defect in ruffle forma-  
724 tion at 2 and 3 days [Figure 1, B and C, *spt8 $\Delta$*  (PC4008),  
725 Figure S3, and Video S7]. The defect was subtle by kymo-  
726 graph analysis but was obvious in the time-lapse analysis. The  
727 *spt8 $\Delta$*  mutant was also defective for colony ruffling and mat  
728 pattern formation (Figure S1). Therefore, we include SAGA  
729 as a regulator of filamentous surface responses in yeast (Fig-  
730 ure 1A, cyan).

### 731 Expression profiling of colony surface growth identifies 732 new targets

733 To explore how filamentation signaling pathways might reg-  
734 ulate surface growth, comparative RNA-seq was performed in  
735 several mutants that disrupt the main pathways that regulate  
736 filamentous growth (dashed blue box in Figure 1A, pathway  
737 diagrams can be found in Figure S4, A–D). RNA was prepared  
738 from wild-type and mutant colonies with the following geno-  
739 types: *ste12 $\Delta$*  (fMAPK), *dig1 $\Delta$*  (fMAPK), *ras2 $\Delta$*  (RAS), *rtg3 $\Delta$*   
740 (RTG), and *spt8 $\Delta$*  (SAGA). RNA was prepared from colonies  
741 under conditions that favored pattern formation (YEP-Gal).  
742 Each mutant showed the expected colony patterning. Specif-  
743 ically, the *ras2 $\Delta$*  (PC562), *rtg3 $\Delta$*  (PC3642), *ste12 $\Delta$*  (PC1079),  
744 and *spt8 $\Delta$*  (PC4008) mutants were less ruffled than wild-type  
745 colonies (PC538), and the *dig1 $\Delta$*  (PC3039) mutant was more  
746

747 ruffled than wild-type colonies (Figure S4E). After sequenc- 803  
748 ing, PCA of the RNA-seq data showed close clustering of 804  
749 strain replicates, while strains differentiated into their repli- 805  
750 cate clusters (Table S1). 806

751 Comparative RNA-seq analysis between the wild-type col- 807  
752 onies and each mutant was performed with the DESeq2 808  
753 package in R (Love *et al.* 2014). Differential gene expression 809  
754 was defined by  $|\log_2FC| > 0.585$  and  $P\text{-value} < 0.01$ . By this 810  
755 method, 1833 genes were differentially expressed in at least 811  
756 one of the mutants tested (Figure S4F) and represented 29% 812  
757 of the ORFs in the genome (Lin *et al.* 2013). The annotated 813  
758 data set can be found in Table S1. To identify the most dif- 814  
759 ferentially regulated targets between the mutant and wild- 815  
760 type colonies, volcano plots showing all differences in gene 816  
761 expression were generated for each mutant. Individual genes 817  
762 were distributed by change in expression ( $x\text{-axis}$ ,  $\log_2FC$ ) and 818  
763 significance of change in expression [ $y\text{-axis}$ ,  $-\log_{10}(P\text{-value})$ ] 819  
764 (Figure 2A). Many of the genes whose expression is 820  
765 known to be induced during filamentous growth were un- 821  
766 covered during the initial analyses (Figure 2A and Table 822  
767 S1). These included targets of the fMAPK pathway: *FLO11* 823  
768 (Rupp *et al.* 1999) (Figure 2A, *dig1Δ* and *ste12Δ*; Table S1, 824  
769 *dig1Δ* and *ste12Δ*), *YLR042C* (Roberts *et al.* 2000) (Figure 825  
770 2A, *ste12Δ*; Table S1, *dig1Δ* and *ste12Δ*), *CLN1* (Madhani 826  
771 *et al.* 1999) (Table S1, *dig1Δ* and *ste12Δ*), *PGU1* (Madhani 827  
772 *et al.* 1999; Roberts *et al.* 2000) (Figure 2A, *dig1Δ* and 828  
773 *ste12Δ*; Table S1, *dig1Δ* and *ste12Δ*), *SVS1* (Roberts *et al.* 829  
774 2000) (Figure 2A, *dig1Δ* and *ste12Δ*; Table S1, *dig1Δ* and 830  
775 *ste12Δ*), *KSS1* (Table S1, *dig1Δ* and *ste12Δ*) (Roberts *et al.* 831  
776 2000), and *MSB2* (Cullen *et al.* 2004) (Table S1, *dig1Δ* and 832  
777 *ste12Δ*). The abovementioned fMAPK pathway targets 833  
778 *YLR042C*, *PGU1* (Roberts *et al.* 2000), *FLO11* (Rupp *et al.* 834  
779 1999) are also *Ras2p*-dependent (Table S1, *ras2Δ*), poten- 835  
780 tially through its regulation of the fMAPK pathway (Mösch 836  
781 *et al.* 1996, 1999; Chavel *et al.* 2010). Similarly, targets of the 837  
782 RTG pathway were identified in the wild-type-*rtg3Δ* data set: 838  
783 *CIT2*, *CIT1*, *IDH1*, *IDH2* (Liu and Butow 1999) (Figure 2A, 839  
784 *rtg3Δ*; Table S1, *rtg3Δ*), and *DLD3* (Liu and Butow 2006) 840  
785 (Table S1, *rtg3Δ*). Genes regulated by SAGA were identified 841  
786 in the wild-type-*spt8Δ* data set [*ADH1*, *ARG1*, *BDF2*, *CTT1*, 842  
787 *FBA1*, *GRE2*, *PGK1*, *TDH3*, and *PHO84* (Basehoar *et al.* 2004; 843  
788 Huisinga and Pugh 2004)] (Table S1, *spt8Δ*). 844

789 Confirmation of other targets by qPCR analysis has been 845  
790 performed in related studies including: targets of fMAPK 846  
791 related to the fungal cell wall, *OCH1*, *PRY2*, *FLO11* and 847  
792  *TIP1* (Chow *et al.* 2018); *SUC2* and *YLR042C* (Chow *et al.*, 848  
793 unpublished data); and *GIC2* (Prabhakar *et al.*, personal com- 849  
794 munication). Therefore, comparative RNA-seq analysis iden- 850  
795 tified many of the genes expected based on previous or 851  
796 parallel studies. 852

797 One question that we sought to address was the extent of 853  
798 target gene overlap among the signaling pathways that reg- 854  
799 ulate filamentous growth. We found that while most genes 855  
800 were regulated by one pathway (Figure S4G, 742/1833 or 856  
801 59%), coregulated targets were seen in almost every combi- 857  
802 nation of regulators, including targets coregulated by all five 858

regulators (Figure S4F). This result also demonstrated that 803  
the SAGA complex coregulated targets with the fMAPK, RAS, 804  
and RTG pathways (Figure S4F), which further validates it as a 805  
major regulator of filamentous growth (Figure 1A, cyan ar- 806  
rows). Additionally, *Spt8p* regulated a target of the *RIM101* 807  
pathway, *NRG1* (Chavel *et al.* 2014) (Figure 1A, cyan arrow), 808  
and a target of lipid biosynthesis, *INO1* (Chavel *et al.* 2014) 809  
(Figure 1A, cyan arrow). SAGA did not coregulate targets of 810  
the *PHO85*, *RPD3(L)*, or ELP pathways. Taken together, these 811  
data suggest that one function of this network of signaling 812  
pathways is to regulate a large number of genes (the more 813  
nodes in the network, the greater the number of differentially 814  
expressed genes); a second function is to coregulate key tar- 815  
gets to amplify target gene expression. 816

817 One possible explanation for the regulatory overlap is cross 817  
818 feedback among the pathways. To explore this aspect of 819  
820 signaling network connectivity, we examined whether genes 821  
822 encoding pathway components were themselves targets of 823  
824 other pathways that regulate filamentous growth. The RTG 825  
826 pathway regulated the expression of components of fMAPK 827  
828 (*MSB2*), RAS (*TPK2*), and SAGA (*SFG73*). fMAPK regulated 829  
830 genes encoding components of its own pathway (*MSB2*, 831  
832 *TEC1*, and *KSS1*) and the RAS pathway (*BCY1*). The RAS 833  
834 pathway regulated one of its own effectors (*TPK1*) and the 835  
836 fMAPK pathway (*TEC1*). SAGA regulated the fMAPK path- 837  
838 way (*MSB2* and *TEC1*) and itself (*SUS1*) (Figure S5, A and B). 839  
840 These results support and extend a previous study, which 841  
842 showed that the activity of the fMAPK is subject to regulation 843  
844 by other filamentation regulatory pathways (Chavel *et al.* 845  
846 2010). Interestingly, not all of the interactions would be 847  
848 expected to result in positive feedback. For example, the 849  
850 *rtg3Δ* mutant showed a  $\sim 1.9$ -fold increase in *TPK2* gene 851  
852 expression (Table S1), which is a PKA subunit and compo- 853  
854 nent of the RAS pathway. These data indicate that coregula- 855  
856 tion of targets may be the result of feedback among the 857  
858 pathways that regulate filamentous growth. 859

859 To identify functionally relevant targets whose expression 860  
861 was amplified by multiple pathways that regulate filamentous 862  
863 growth, we focused on genes that were differentially 864  
865 expressed in all regulatory mutants (Figure 2B and Table 866  
867 S2, all mutants). GO term analysis (Ashburner *et al.* 2000) 868  
869 of the coregulated genes showed significant enrichment in 869  
870 cell adhesion, cell wall constituents, and fungal cell wall pro- 871  
872 teins (Table S2, all mutants). One of the targets that was 873  
874 coregulated by all five regulators, and that was included in 875  
876 many of the above enriched GO terms, was the gene that 877  
878 encodes the major cell adhesion molecule *Flo11p* (Figure 879  
880 2B and Table S2, all mutants). *FLO11* is known to be regu- 881  
882 lated by a large number of proteins and pathways (Rupp *et al.* 883  
884 1999; Barrales *et al.* 2008). We confirmed that fMAPK, RAS, 885  
886 RTG, and *Spt8p* controlled *FLO11* expression by qPCR (Fig- 887  
888 ure 2C). These data fit with the key role that *Flo11p* plays in 889  
890 regulating adhesion-dependent responses in yeast. Another 891  
892 target regulated by all five mutants, which also had the larg- 893  
894 est net change in regulation, was *PGU1*, the gene that en- 895  
896 codes a secreted pectinase that is also expressed during 897  
898 899 900



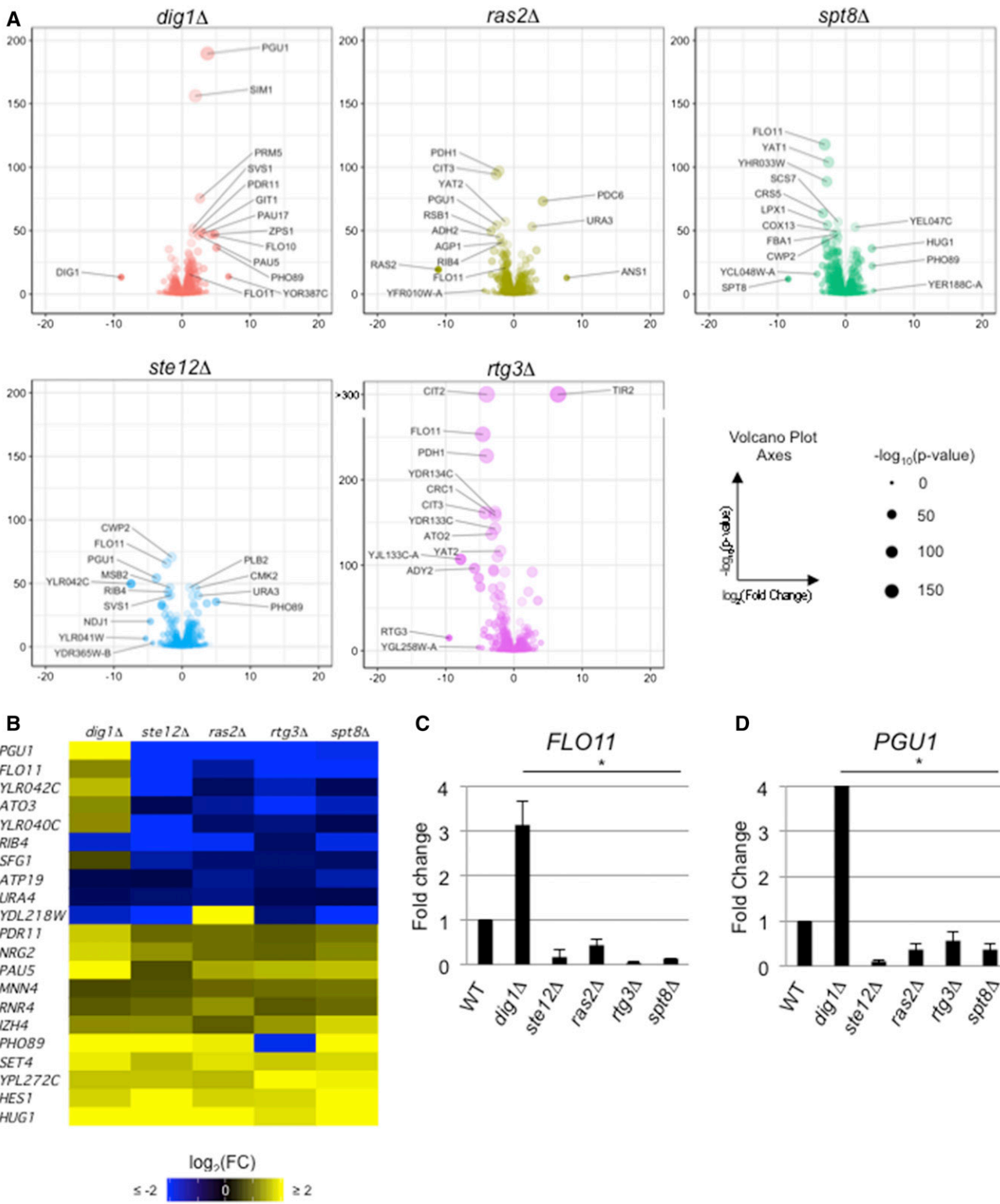


**Figure 2** Comparative RNA-seq analysis identifies common and unique targets of signaling pathways that regulate filamentous growth. (A) Volcano plots showing comparative RNA-seq between the indicated mutant and WT. Dot size is  $-\log_{10}(P\text{-value})$ . Volcano plot x-axis is  $\log_2(\text{FC})$ ; y-axis is  $-\log_{10}(P\text{-value})$ . Labeled dots are 10 targets with lowest  $P$ -value or five targets with highest lfold change. *FLO11* has also been labeled on *dig1Δ* and *ras2Δ* plots. *CIT2* and *TIR2* have calculated  $P$ -values  $< 10^{-300}$  in the *rtg3Δ* mutant, as reflected in the break in the y-axis. (B) Heat map showing targets with  $|\log_2(\text{FC})| > 0.585$  and  $P\text{-value} < 10^{-3}$ . (C) Bar graph showing fold change in *FLO11* mRNA levels, normalized to *ACT1* with WT values set to 1, in the indicated mutants by qPCR analysis by the  $\Delta\Delta\text{Ct}$  quantitation method. The experiment was performed in triplicate and error bars represent the SD between experiments. \*  $P < 0.05$  for all differences compared to WT. (D) Bar graph showing fold change in *PGU1* mRNA levels. See (C) for details.  $\log_2(\text{FC})$ ,  $\log_2(\text{Fold Change})$ ; qPCR, quantitative PCR; RNA-seq, RNA sequencing; WT, wild-type.

971  
972  
973  
974  
975  
976  
977  
978  
979  
980  
981  
982  
983  
984  
985  
986  
987  
988  
989  
990  
991  
992  
993  
994  
995  
996  
997  
998  
999  
1000  
1001  
1002  
1003  
1004  
1005  
1006  
1007  
1008  
1009  
1010  
1011  
1012  
1013  
1014  
1015  
1016  
1017  
1018  
1019  
1020  
1021  
1022  
1023  
1024  
1025  
1026

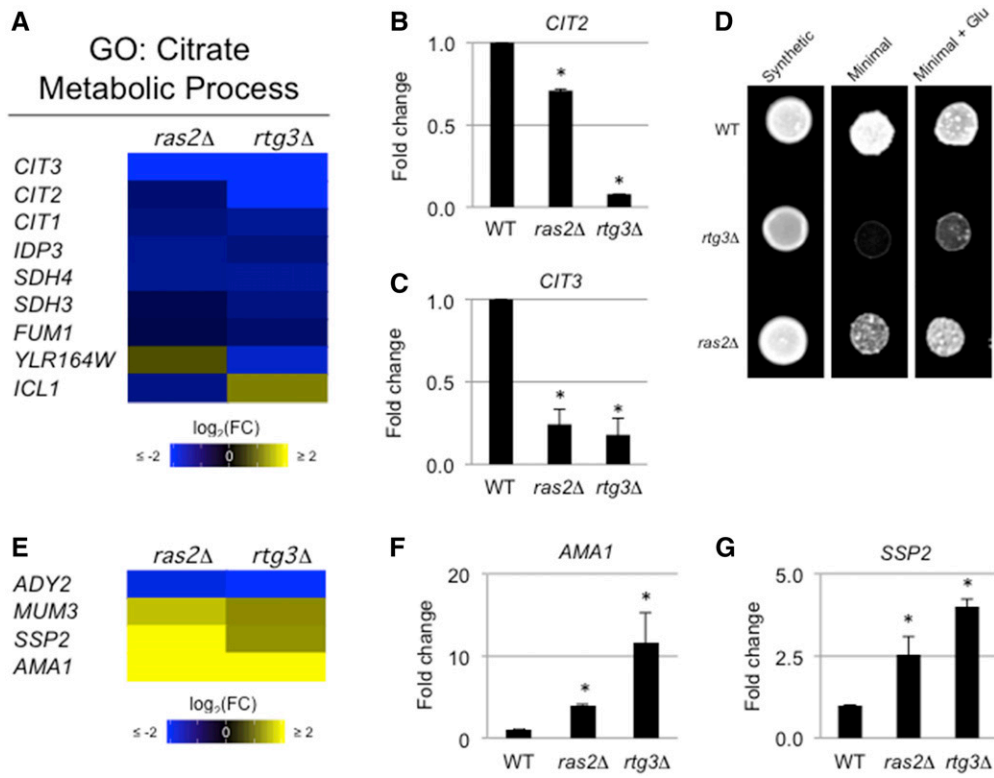


**Figure 3** Common and unique target genes of the RAS and RTG pathways. (A) Heat map of targets coregulated by the RAS and RTG pathways with the citrate metabolic process GO term. (B and C) Bar graph showing fold change in (B) *CIT2* and (C) *CIT3* mRNAs in *ras2Δ* and *rtg3Δ* relative to WT. See Figure 2C for details. (D) Strains spotted onto synthetic media, minimal media, or minimal media with glutamate. Cells were grown for 48 hr. (E) Heat map of targets coregulated by RAS and RTG associated with sporulation. (F and G) Bar graphs showing fold change in (F) *AMA1* and (G) *SSP2* mRNAs in *ras2Δ* and *rtg3Δ* relative to WT. See Figure 2C for details. Glu, glutamate; GO, gene ontology; log<sub>2</sub>(FC), log<sub>2</sub>(Fold Change); WT, wild-type.

1027  
1028  
1029  
1030  
1031  
1032  
1033  
1034  
1035  
1036  
1037  
1038  
1039  
1040  
1041  
1042  
1043  
1044  
1045  
1046  
1047  
1048  
1049  
1050  
1051  
1052  
1053  
1054  
1055  
1056  
1057  
1058  
1059  
1060  
1061  
1062  
1063  
1064  
1065  
1066  
1067  
1068  
1069  
1070  
1071  
1072  
1073  
1074  
1075  
1076  
1077  
1078  
1079  
1080  
1081  
1082

filamentous growth (Madhani *et al.* 1999; Cullen 2015a). This result was confirmed by qPCR analysis (Figure 2D). Taken together, our results are consistent with the idea that multiple signaling pathways and protein complexes coordinately regulate target gene expression during colonial surface growth (Figure 2A). One function of the network is to control the expression of *FLO11*, a major regulator of adhesion-dependent responses in yeast (Figure 2, B and C).

**A regulatory connection between the RAS and RTG pathways**

In an analysis of highly significant changes in expression in the *ras2Δ* and *rtg3Δ* sets ( $P < 10^{-12}$ ) (Figure S6), 41 targets were in common and 93% of these targets (39/41) showed the same regulation (both up or down) (Figure S6). For example, citrate synthase, *CIT3*, was among the significant, differentially expressed genes in both *ras2Δ* and *rtg3Δ* (Figure 2A). Other citrate synthases, *CIT1* and *CIT2*, were also coregulated by both the *ras2Δ* and *rtg3Δ* mutants (Figure 3A and Table S1). We confirmed that RAS and RTG coregulated *CIT2* and *CIT3* by qPCR analysis (Figure 3, B and C). Because of the extent of coregulation, especially the coregulation of all citrate synthase isoforms (Graybill *et al.* 2007), the full set of RAS and RTG coregulated targets was examined further.

As expected, the RTG pathway regulated mitochondrial gene targets (Table S1). Many of the genes were also regulated by the RAS pathway (Table S1; *PDH1*, *YAT1*, and *YAT2*) (Schmalix and Bandlow 1993; Epstein *et al.* 2001; Swiegers *et al.* 2001). Moreover, several hallmark RTG targets were also regulated by the RAS pathway (Table S1; *CIT1*, *CIT2*,

*CIT3*, *ATO2*, and *ATO3*) (Suissa *et al.* 1984; Kim *et al.* 1986). In addition to coregulation of cell wall components (*i.e.*, *FLO11*), GO term analysis identified significant enrichment of the citrate metabolic process by the overlapping RAS and RTG targets (Figure 3A and Table S2), and the citric acid cycle (Figure S7). Because RAS and RTG coregulated genes that are involved in the citric acid cycle, we hypothesized that RAS might be required to support that mitochondrial role. The mitochondria are critical for glutamate biosynthesis (Liu and Butow 1999; Magasanik and Kaiser 2002) and RTG is required for growth in medium lacking glutamate [Figure 3D, *rtg3Δ* (Liao and Butow 1993; Small *et al.* 1995; Chavel *et al.* 2014)]. More specifically, a loss of citrate synthases results in glutamate auxotrophy in *S. cerevisiae* (Kim *et al.* 1986), so we hypothesized that a RAS pathway mutant would be sensitive to limiting glutamate. Like RTG, the RAS pathway was also required for growth in this condition (Figure 3D, *ras2Δ*). The growth defects of cells lacking an intact RAS or RTG pathway were bypassed by the addition of glutamate (Figure 3D). Therefore, the RAS pathway plays a role in this mitochondrial process.

Similarly, the RAS pathway regulated genes that are required for sporulation (Table S1) and a subset of these genes were coregulated by the RTG pathway [Figure 3E, *ADY2* (Rabitsch *et al.* 2001), *AMA1* (Coluccio *et al.* 2004), *SSP2* (Sarkar *et al.* 2002), and *MUM3* (Engbrecht *et al.* 1998)]. Several of the genes were confirmed by qPCR analysis (Figure 3, F and G). Therefore, the RAS and RTG pathways coregulate functionally related genes and may be more functionally connected than has been previously thought.

1083  
1084  
1085  
1086  
1087  
1088  
1089  
1090  
1091  
1092  
1093  
1094  
1095  
1096  
1097  
1098  
1099  
1100  
1101  
1102  
1103  
1104  
1105  
1106  
1107  
1108  
1109  
1110  
1111  
1112  
1113  
1114  
1115  
1116  
1117  
1118  
1119  
1120  
1121  
1122  
1123  
1124  
1125  
1126  
1127  
1128  
1129  
1130  
1131  
1132  
1133  
1134  
1135  
1136  
1137  
1138

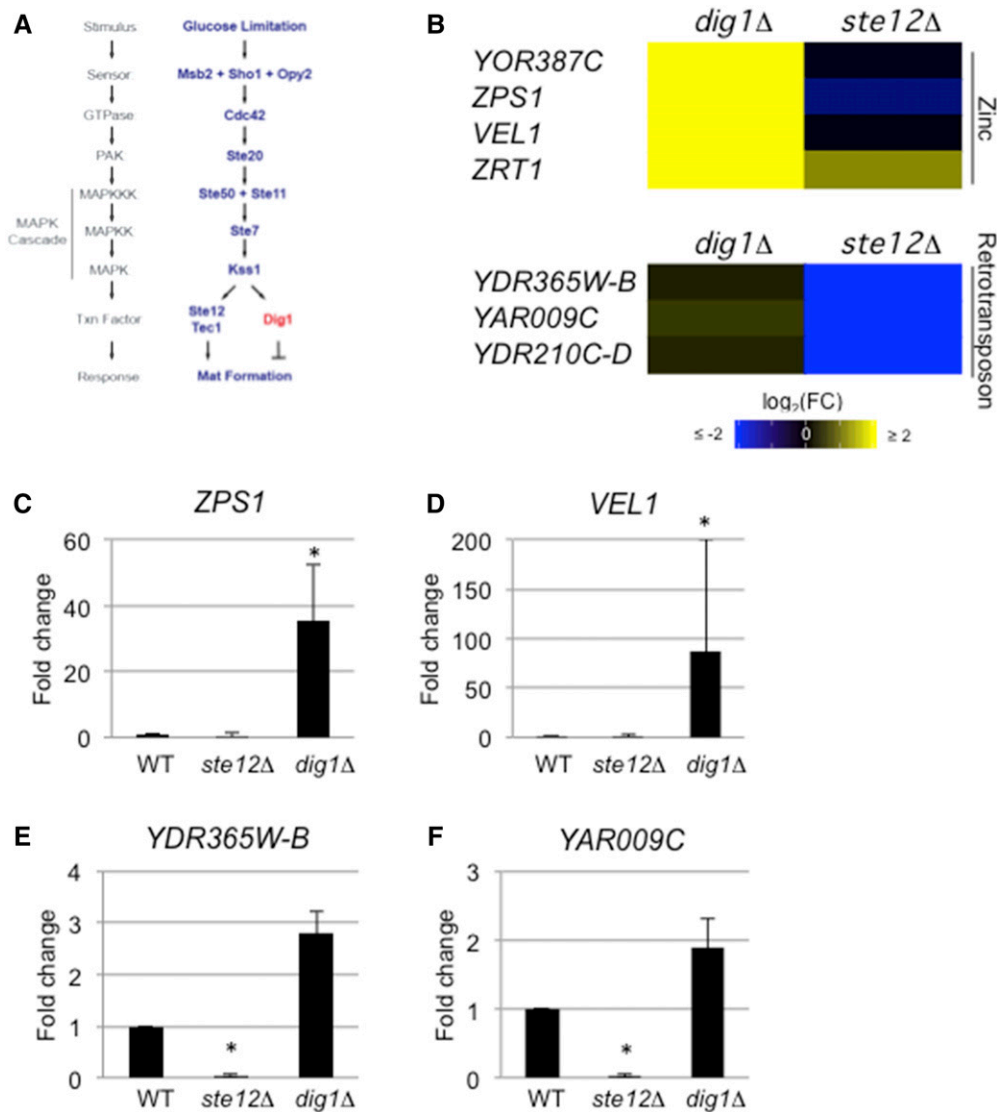


**Figure 4** Common and unique genes regulated by Ste12p and Dig1p. (A) Model of the fMAPK pathway showing Ste12p and Dig1p. (B) Heat map of indicated targets regulated in the *dig1Δ* or *ste12Δ* mutants. (C–F) Bar graphs showing fold change in target mRNA levels for (C) *ZPS1*, (D) *VEL1*, (E) *YDR365W-B*, and (F) *YAR009C*. See Figure 2C for details. fMAPK, fungal MAPK;  $\log_2(\text{FC})$ ,  $\log_2(\text{Fold Change})$ ; WT, wild-type.

1139  
1140  
1141  
1142  
1143  
1144  
1145  
1146  
1147  
1148  
1149  
1150  
1151  
1152  
1153  
1154  
1155  
1156  
1157  
1158  
1159  
1160  
1161  
1162  
1163  
1164  
1165  
1166  
1167  
1168  
1169  
1170  
1171  
1172  
1173  
1174  
1175  
1176  
1177  
1178  
1179  
1180  
1181  
1182  
1183  
1184  
1185  
1186  
1187  
1188  
1189  
1190  
1191  
1192  
1193  
1194

**Nonreciprocal target genes are regulated by opposing transcriptional regulators of the fMAPK pathway**

*Ste12p* is one of the transcription factors that regulates the fMAPK pathway (Liu *et al.* 1993). The transcriptional repressor *Dig1p* inhibits *Ste12p*-dependent transcription (Cook *et al.* 1996; Tedford *et al.* 1997; Bardwell *et al.* 1998; Olson *et al.* 2000; Breitzkreutz *et al.* 2003; Kusari *et al.* 2004; Chou *et al.* 2006; van der Felden *et al.* 2014). Although the transcriptional outputs of the pathway can be complex resulting in nonuniform target gene regulation (Breitzkreutz *et al.* 2003), *Ste12p* and *Dig1p* were expected to regulate a common set of targets in a reciprocal manner (Figure 4A). We unexpectedly found that the pattern of gene regulation by the two proteins could not be solely explained by reciprocal regulation. In an analysis of the most significant changes in expression in the *dig1Δ* and *ste12Δ* sets ( $P < 10^{-12}$ ) (Figure S8), 20 targets were found to be in common and only 50% (10/20) were reciprocally regulated (up in *dig1Δ* and down in *ste12Δ*) (Figure S8). As expected, *Ste12p* and *Dig1p*

showed reciprocal regulation of a subset of target genes (Figure S8; *FLO11/MUC1*, *PGU1*, *YLR042C*, and *BARI*). However, more genes were independently regulated only by *Dig1p* or only by *Ste12p* (Figure S8).

For example, the target with the largest change in expression identified in the *dig1Δ* volcano plot was *YOR387C* (> 111-fold increase) (Figure 2A and Table S1). Although *YOR387C* lacks associated GO terms, a literature search indicated that *YOR387C* is induced in zinc-limiting conditions (Higgins *et al.* 2003; Wu *et al.* 2008). Although *YOR387C* and its paralog *VEL1* (Higgins *et al.* 2003) were significantly regulated in the *dig1Δ* mutant, neither gene was found to be regulated in the *ste12Δ* mutant (Figure 4B and Table S1). Additionally, only the *dig1Δ* mutant showed a change in expression of *ZAP1* (Table S1), a major transcription factor induced by limiting zinc (Zhao and Eide 1997). Interestingly, the ability of cells to take up trace zinc was determined to be critical for flocculation (Yuan 2000), which is a closely related response to filamentous growth and mat formation. A

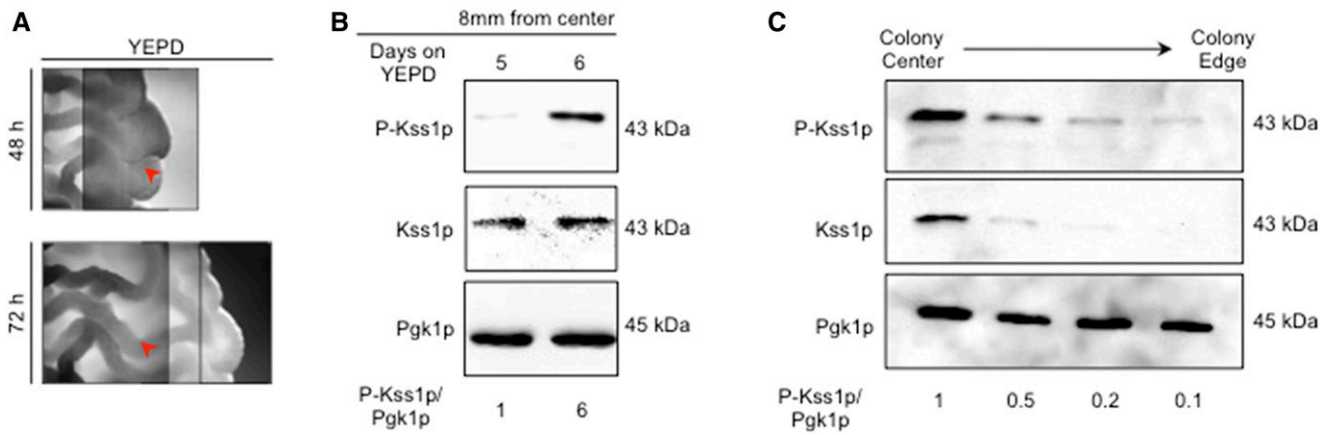


**Figure 5** Different ruffling patterns in colonies correspond to different levels of fMAPK pathway activity. (A) Bright-field microscopy of a wild-type colony grown in YEPD for 48 and 72 hr. Red arrow indicates same location on a mat at 48 hr when the region is smooth and 72 hr when the region has become ruffled. Different focal planes of the same colony are shown. (B) Immunoblot analysis using p42/p44 antibodies to detect P-Kss1p levels from extracts prepared from cells before and after ruffling. Immunoblots were also performed using antibodies to Kss1p and Pgk1p as loading controls. (C) Immunoblot analysis using p42/p44 antibodies to detect phosphorylated Kss1p at different parts of a colony. Immunoblots were also performed using antibodies to Kss1p and Pgk1p as loading controls. fMAPK, fungal MAPK; YEPD, yeast extract, peptone, and dextrose.

subset of other upregulated targets in the *dig1Δ* mutant were genes induced under low-zinc conditions [Figure 4B, *ZPS1* (Lyons *et al.* 2000)] as well as a zinc transporter [*ZRT1* (Zhao and Eide 1996)]. These genes were not strongly downregulated in the *ste12Δ* mutant. The expression profiles of *ZPS1* and *VEL1* were confirmed by qPCR analysis (Figure 4, C and D).

Likewise, the *ste12Δ* mutant showed downregulation of some target genes that were not altered in the *dig1Δ* mutant. One of the targets identified in the *ste12Δ* volcano plot was the retrotransposon *YDR365W-B* (Kim *et al.* 1998). Other retrotransposons—*YDR365W-B*, *YOL103W-B*, *YAR009C*, and *YDR210C-D* (Kim *et al.* 1998)—were also regulated by *Ste12p* but less so by *Dig1p* (Figure 4B). The expression profiles of *YDR365W-B* and *YAR009C* were confirmed by qPCR analysis (Figure 4, E and F). Thus, key transcriptional regulators of the fMAPK pathway operate through mechanisms that do not only involve reciprocal regulation between the two proteins.

#### Changes in colony patterning correspond to changes in MAPK pathway activity

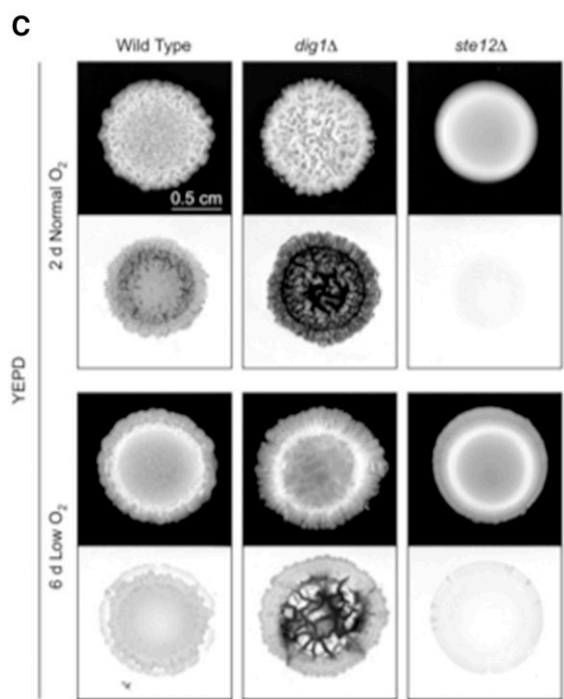
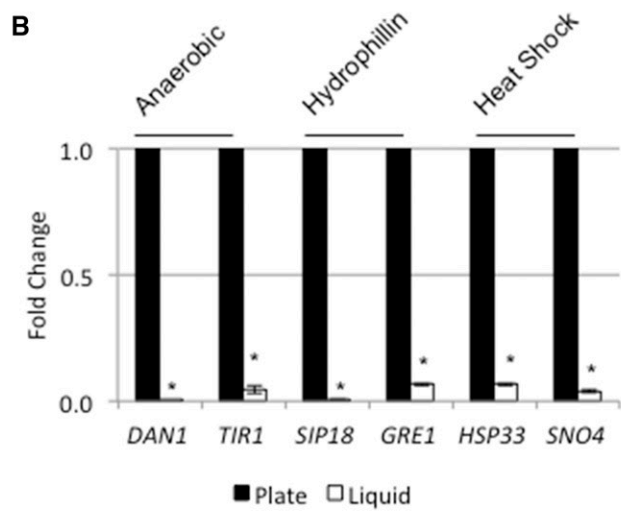
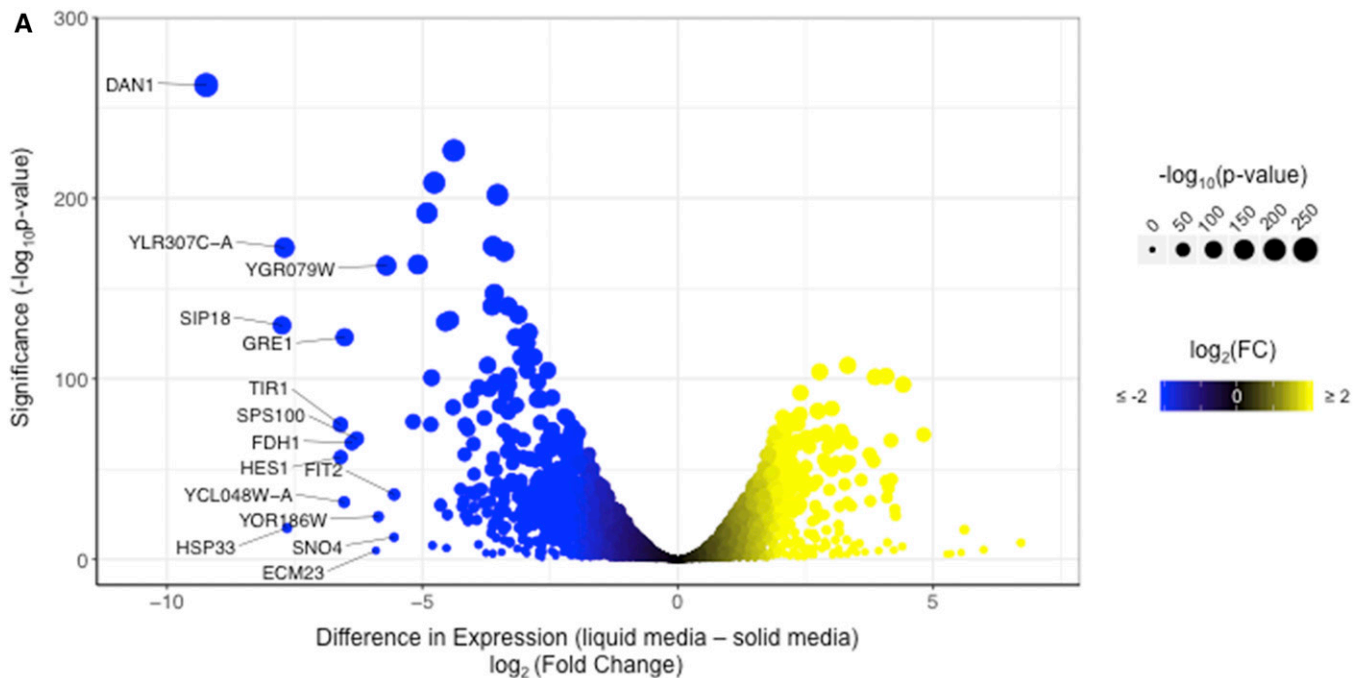
We also examined the development of colony pattern formation under different conditions and over time. Colonies showed different ruffling patterns under different conditions. For example, growth in preferred carbon sources such as glucose media (YEPD) resulted in colony perimeters that were smooth compared to a ruffled colony interior (Figure 5A, adjacent photographs of a colony are shown at different focal planes on the *z*-axis). Such differences were not observed in more uniformly ruffled colonies grown on a nonpreferred carbon source (YEP-Gal) (Video S1). Over time, the smooth regions of the colony became ruffled (Figure 5A, red arrow marks the same location in the colony).

One explanation for differences in colony pattern formation might be that different parts of the colony are exposed to

different environments. The fMAPK pathway, which is sensitive to nutrient levels, may induce different responses in different parts of the colony. To test this possibility, samples from regions of the colony were collected and examined for fMAPK activity by phosphorylation of the MAP kinase *Kss1p* (Cullen 2015a). Samples collected from smooth colony perimeters showed low P~*Kss1p* levels (day 5, smooth). Samples collected from the same physical location that had become ruffled (day 6, ruffled) showed high P~*Kss1p* levels (Figure 5B). This result indicates that as cells in colonies consume nutrients and subsequently starve, the fMAPK pathway is activated to promote ruffle formation. In line with this possibility, colony interiors showed higher levels of P~*Kss1p* compared with colony perimeters (Figure 5C). We note that in this experiment, the levels of total *Kss1p* protein were also lower at colony perimeters. *KSS1* is a target of the fMAPK pathway, and the regulation of total *Kss1p* may be a way that fMAPK regulates its activity through positive feedback (Roberts *et al.* 2000). Therefore, signaling pathways may exhibit different activities, and induce target genes to different levels, in a manner that is influenced by nutrient levels (and time) to control adhesion-dependent surface growth.

#### Genes that respond to oxygen, desiccation, and temperature stress were induced during colony surface growth

Growth on surfaces presents unique challenges compared to the uniform growth in liquid cultures. To further explore the response to colonial growth on surfaces, expression profiling data sets were compared between cells grown in liquid (Adhikari and Cullen 2014) and cells grown on an agar surface (this study). Growth on surfaces caused the differential expression of 3267 genes when compared to growth in liquid (Table S1, wild-type liquid–solid,  $|\log_2FC| > 0.585$  and  $FDR < 0.05$ ). This represents ~54% of the yeast genome



**11** **Figure 6** Target genes induced during surface growth correspond to the response to specific stresses. (A) Volcano plot showing the difference in expression and significance of all targets between growth in liquid media vs. solid media. x-axis is  $\log_2(\text{Fold Change})$ ; y-axis is  $-\log_{10}(P\text{-value})$ . Labeled targets are the top 15 induced targets during surface growth. (B) Relative fold change of the indicated gene was determined by qPCR analysis. Expression normalized to *ACT1* in the indicated mutants, as determined by qPCR analysis. The experiment was performed in triplicate and error bars represent the standard difference between experiments. \*  $P < 0.05$  for differences compared to wild-type. (C) Wild-type cells and the indicated mutants were spotted on YEPD 2% agar media in normal and low-oxygen conditions. Colonies were grown for the indicated times to compare colony patterns and invasive growth. Inverted images of the invasive scars are shown.  $\log_2(\text{FC})$ ,  $\log_2(\text{Fold Change})$ ; qPCR, quantitative PCR; YEPD, yeast extract, peptone, and dextrose.

[6091 genes (Lin *et al.* 2013)]. Functional classification of the top 15 induced targets (Figure 6A, >25-fold increase in expression) during surface growth included genes induced during anaerobic stress [*DAN1* (Sertil *et al.* 1997) and *TIR1* (Cohen *et al.* 2001), Figure 6A], desiccation/dehydration [*SIP18* (Miralles and Serrano 1995) and *GRE1* (Garay-Arroyo and Covarrubias 1999), Figure 6A], and elevated temperature [*HSP33* (Wilson *et al.* 2004) and *SNO4* (Samanta and Liang 2003), Figure 6A]. An expanded list of the top 50 (>15-fold increase in expression) induced targets included genes that regulate metal homeostasis, RNA processing, and the metabolism of lipids and nonfermentable carbon sources, as well as genes of unknown function (Figure S9).

The most differentially induced target during surface growth was the gene that encodes the anaerobic-responsive cell wall mannoprotein *Dan1p* (Mrsa *et al.* 1999) (Figure 6A). qPCR analysis showed that *DAN1* expression was induced during surface growth (Figure 6B). Examination of the *dan1Δ* mutant from an ordered gene deletion collection (Ryan *et al.* 2012) showed a defect in colony ruffling (Figure S10, *dan1Δ*). Thus, *Dan1p* may impact colony patterning in response to stresses associated with surface growth. In addition to *DAN1*, the four members of the Tir family of anaerobic-responsive cell wall mannoproteins (Cohen *et al.* 2001) also showed transcriptional induction during surface growth (Figure 6A and Table S1, wild-type liquid–solid), which was verified in a study on the regulation of the cell wall (Chow *et al.* 2018). Therefore, anaerobic-specific changes to the cell wall also occur during surface growth in yeast.

Because targets that encode anaerobic-responsive proteins were among the top induced targets during colony surface growth [*DAN1* and the *TIR* genes (Figure 6A)], the impact of oxygen in colony ruffling and invasive growth was examined. *S. cerevisiae* undergoes aerobic alcohol fermentation by what is known as the Crabtree effect (Crabtree 1929). In yeast, this includes the repression of genes involved in aerobic respiration in the presence of glucose during exponential growth (De Deken 1966). Studies that explore this phenomenon in yeast have done so in liquid culture (De Deken 1966; Hagman *et al.* 2014), but the role of oxygen in regulating aspects of colonial growth has not been explored. To determine the role of oxygen on colony pattern formation, wild-type and *dig1Δ* colonies grown in normal atmospheric oxygen (20% oxygen) were compared to colonies grown in low oxygen (5–15% oxygen). Comparing the colonies at similar sizes (2-day normal oxygen and 6-day low oxygen) showed that both were less ruffled in low oxygen (Figure 6C). Wild-type and *dig1Δ* colonies showed reduced invasive growth in low oxygen (Figure 6C). Additionally, wild-type, *dig1Δ*, and *ste12Δ* colonies grown in limiting oxygen (5–15% oxygen or 0% oxygen) grew more slowly than in normal oxygen (20% oxygen) (Figure S11). Slower growth was not bypassed with excess glucose (Figure S11, 8% Glu) as might be predicted by the Crabtree effect in yeast. Therefore, oxygen levels impact colony patterning and invasive growth.

Another class of genes induced during surface growth has been described as regulated during desiccation. These included the gene that encodes the hydrophilin *Sip18p* (Miralles and Serrano 1995; Dang and Hinch 2011) (Figure 6A). A second hydrophilin, *Gre1p*, (Garay-Arroyo and Covarrubias 1999) was also among the top 10 induced targets (Figure 6A). Four of six hydrophilins and putative hydrophilins were induced during surface growth (Table S1, wild-type liquid–solid). Hydrophilins such as *Sip18p* allow for survival under desiccation stress and during the dehydration/rehydration process (Rodríguez-Porrata *et al.* 2012). The induction of hydrophilin-encoding genes *SIP18* and *GRE1* during surface growth was confirmed by qPCR analysis (Figure 6B). By testing mutants from an ordered deletion collection (Ryan *et al.* 2012), we found that the loss of either hydrophilin, *SIP18* or *GRE1* (Figure S10A; *gre1Δ* and *sip18Δ*), increased mat ruffling and hyper-invasive growth, indicating that intracellular hydration may be a trigger for both invasive growth and colony ruffling (Figure S10B; *gre1Δ* and *sip18Δ*). Therefore, cells in mats may experience desiccation stress, and genes induced under this condition can impact colony patterning.

Genes encoding the heat-shock proteins *Hsp33p* (fourth most-induced target), *Sno4p*, *Hsp26p*, and *Hsp12p* were also induced during mat growth. Additionally, as shown below, a ruffled colony showed a temperature differential of 0.8° between its warmest and coolest regions (see Figure 7D, below). Modest differences in temperature have previously been shown to effect metabolism in *S. cerevisiae* (Jones and Hough 1970). *Spg4p*, described as being essential for growth at high temperature (Martinez *et al.* 2004), was also among the top targets. Using an ordered deletion collection, we explored the roles of *SNO4* and *HSP26* (Bentley *et al.* 1992) (Figure S10A; *sno4Δ* and *hsp26Δ*), as the *hsp33Δ* mutant did not exist in the deletion collection. Deletion of either of these genes resulted in smoother colonies.

None of the mutants tested were necessary for growth in low-oxygen (5–15% O<sub>2</sub>), high-temperature (37°), or desiccated conditions (Figure S11). This may be a result of functional redundancy among the major induced targets. Taken together, oxygen, temperature, and desiccation stresses impact colonial growth in yeast. Genes induced during surface growth impact colony patterning that may aid in the response to these stresses.

#### ***Flo11p-dependent adhesion protects cells in colonies from a nematode predator***

*Flo11p* is an established regulator of filamentous growth, and its role in maintaining contacts between cells to form filaments has obvious benefits during surface penetration (e.g., invasive growth) into new environments. However, the broader functional implications of *Flo11p*-dependent adhesion between cells on the colony surface are not clear. The interactions among yeast cells mediated by a related flocculin, *Flo1p*, can provide protection from toxins and antibiotics (Smukalla *et al.* 2008), and cell adhesion has more generally

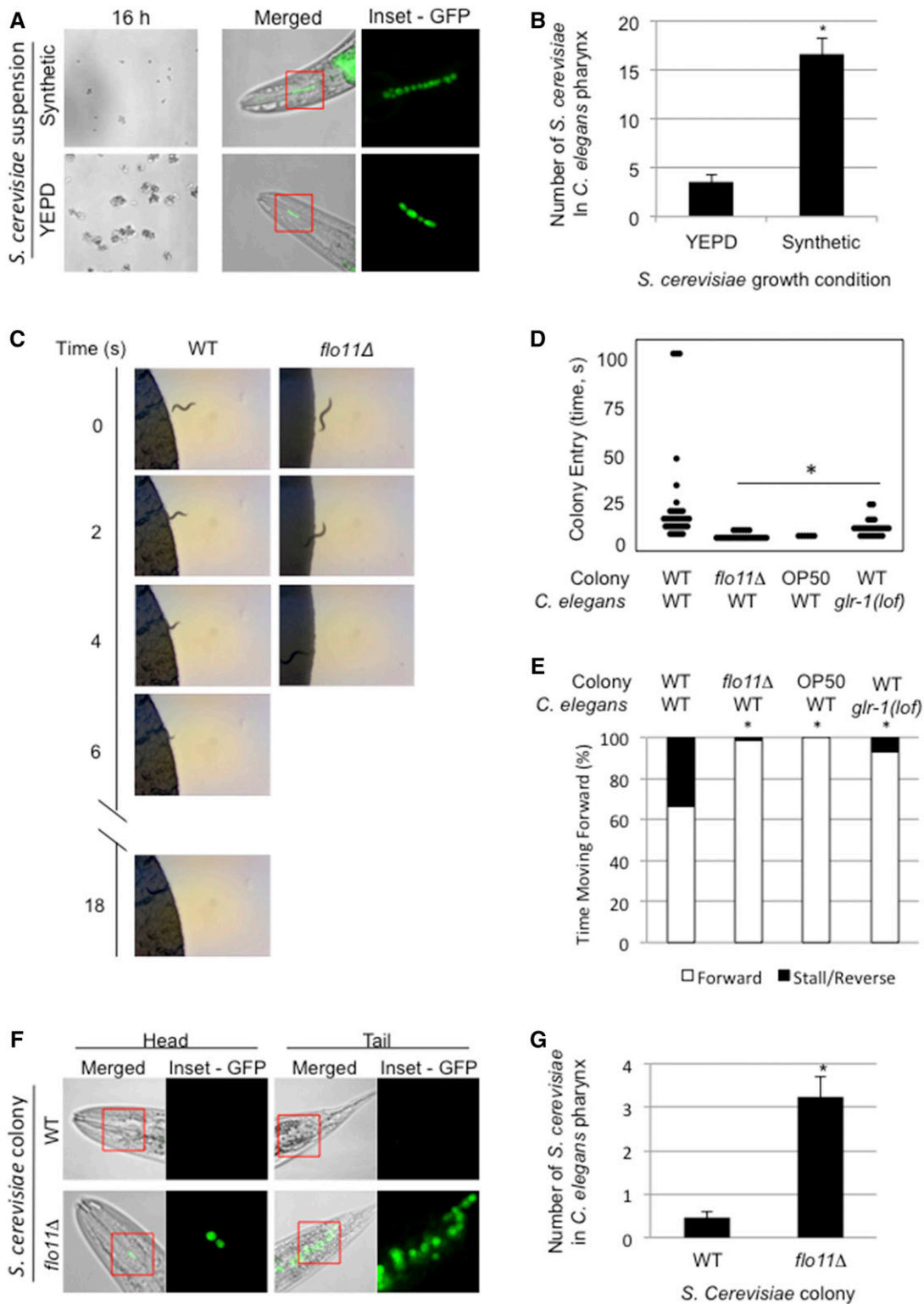


**Figure 7** Impact of Flo11p on predator avoidance in yeast colonies. (A) Suspensions of GFP-labeled WT cells (PC6733) grown for 16 hr in synthetic or YEPD media (16 hr). Merged fluorescent and brightfield images of heads of mounted *C. elegans* showing fluorescent *S. cerevisiae* inside the animal pharynx after 45 min feeding (merged). Fluorescent images of individual *S. cerevisiae* inside the animal pharynx (inset = GFP). (B) Bar graph showing difference in average number of *S. cerevisiae* cells in *C. elegans* pharynx between YEPD- and synthetic-grown suspensions. Error bars are SE. \*  $P < 0.05$ . (C) Selected images from videos showing WT *C. elegans* entering WT or *flo11Δ* yeast colonies. A set of representative videos are available in the supplement (Videos S8–S15). (D) Dot plot showing the time required for worms to enter the indicated colonies. WT (N2) or *glr-1(lof)* *C. elegans* worms were placed on plates containing WT or *flo11Δ* yeast, or the *E. coli* food strain OP50. (E) Stacked bar graphs comparing *C. elegans* forward movement to stalls and/or reversals in the indicated yeast or *E. coli* colonies. (F) Three-day-old colonies of WT (PC538) and *flo11Δ* (PC1029) cells expressing-plasmid

1643 been postulated to provide protection to individual cells of a  
1644 colony (Granek and Magwene 2010). In bacterial communi-  
1645 ties, the growth of cells in mats can deter predation by other  
1646 microbes and multicellular predators, like nematodes (Darby  
1647 *et al.* 2002). To explore whether cell adhesion contacts might  
1648 similarly protect fungal cells from predation, we developed a  
1649 mock predator–prey assay between *S. cerevisiae* and the nem-  
1650 atode *C. elegans*.

1651 *C. elegans* is a free-living nematode that is commonly used  
1652 in research laboratories (Brenner 1974), and has been used  
1653 to study the effects of *C. albicans* and *S. cerevisiae* accumula-  
1654 tion in the gut (Jain *et al.* 2009; Bois *et al.* 2013). *C. elegans*  
1655 feed on bacteria and other microbes including yeasts (Félix  
1656 and Braendle 2010). The pharynx, a neuromuscular pump,  
1657 contracts and relaxes rhythmically to draw in liquid and sus-  
1658 pended particles to grind them up before transporting them  
1659 to the intestine. Although the pharynx pumps continuously,  
1660 previous studies have shown that microbe size is a determin-  
1661 ing factor in *C. elegans* feeding; large food is often excluded  
1662 during this grazing behavior (Avery and Shtonda 2003;  
1663 Shtonda and Avery 2006; Fang-Yen *et al.* 2009). One function  
1664 of cell adhesion molecules is to allow cells to adhere to each  
1665 other, leading to large colonies. To observe the impact of such  
1666 adhesion, wild-type *S. cerevisiae* cells were grown in condi-  
1667 tions that either permit cell–cell adherence (Figure 7A, YPD)  
1668 or suppress adherence (Figure 7A, synthetic). *C. elegans* were  
1669 transferred into suspensions of *S. cerevisiae* as per established  
1670 methods (Bois *et al.* 2013). We found that less-adherent *S.*  
1671 *cerevisiae* (Figure 7A, synthetic) were taken into the pharynx  
1672 of *C. elegans* in greater numbers than *S. cerevisiae* that ad-  
1673 hered to each other (Figure 7A, YPD). This finding is consis-  
1674 tent with the idea that cell–cell adhesion protects cells from  
1675 ingestion by *C. elegans*.

1676 We next assessed how yeast cells growing in adhesive  
1677 colonies might impact the feeding behavior of *C. elegans*.  
1678 To test this possibility, the time required for worms to pene-  
1679 trate yeast colonies from nose to tail was measured for  $\leq$   
1680 100 sec (Figure 7, C and D and Videos S8–S15). Worm stall-  
1681 ing and reversing out of the colony was also examined (Fig-  
1682 ure 7E). After 3 days of colony growth, a wild-type yeast  
1683 strain that formed normal, ruffled colonies slowed *C. elegans*  
1684 as it attempted to penetrate the colony (Figure 7, C–E, and  
1685 Videos S8 and S9). In some cases, worms abandoned enter-  
1686 ing the colony entirely. In contrast, a *flo11Δ* colony, which  
1687 fails to form ruffled colonies, did not deter worms from enter-  
1688 ing (Figure 7, C–E, and Videos S10 and S11). *flo11Δ* col-  
1689 onies were equally vulnerable to nematode entry as a colony  
1690 of OP50, an *E. coli* laboratory food strain for *C. elegans*  
1691 (Brenner 1974) (Figure 7, D and E, and Videos S12 and  
1692 S13). Additionally, *C. elegans* transferred directly into  
1693 *flo11Δ S. cerevisiae* colonies ingested more cells than *C. ele-*

1699 *gans* transferred into wild-type *S. cerevisiae* colonies (Figure  
1700 7, F and G). It is important to note here that our results out-  
1701 line an association between a lack of physical barrier and a  
1702 higher rate of being consumed by *C. elegans*. As such, we  
1703 expect any mutant that lacks the physical barrier conferred  
1704 by adhesive colonies would be similarly vulnerable.

1705 *C. elegans* might be excluded from wild-type colonies due  
1706 to the physical barrier encountered by wild-type colonies  
1707 expressing *FLO11*. Additionally, exclusion might also result  
1708 from a change in a worm’s sensory response to the colony  
1709 surface. Wild-type *C. elegans* halt their forward locomotion  
1710 and initiate backward movement in response to a light touch  
1711 to their anterior-most tip (nose). This avoidance of touch to  
1712 the worm’s nose has been termed the nose-touch response  
1713 (Kaplan and Horvitz 1993), a behavior involving the ASH <sup>10</sup>  
1714 polymodal nociceptive sensory neurons (with a small contri-  
1715 bution from the FLP and OLQ sensory neurons) (Kaplan and  
1716 Horvitz 1993). The glutamate-gated ion channel GLR-1 func-  
1717 tions in the downstream command interneurons and is re-  
1718 quired for the nose-touch response (Hart *et al.* 1995; Maricq  
1719 *et al.* 1995). To test the possibility that *C. elegans* do not  
1720 effectively enter yeast colonies due to the activation of this  
1721 mechanosensory avoidance response, experiments were per-  
1722 formed with *C. elegans glr-1(n2461)* loss-of-function (*lof*)  
1723 mutant animals, which are defective for nose touch, exposed  
1724 to a wild-type yeast colony. The *glr-1(lof)* mutant animals  
1725 penetrated colonies faster than wild-type worms, though this  
1726 was still slower than wild-type worms penetrating *flo11Δ*  
1727 yeast colonies (Figure 7D, and Videos S14 and S15). In ad-  
1728 dition, the *glr-1(lof)* mutant animals had fewer stalls and  
1729 reversals upon initial colony entry than wild-type *C. elegans*  
1730 (Figure 7E). Taken together, our data reveal a clear associa-  
1731 tion between the formation of adhesive contacts between  
1732 yeast cells in surface-growing colonies and predation in a  
1733 laboratory setting, both by becoming too large to eat and also  
1734 by forming a physical barrier. Further experiments are  
1735 needed to establish if protection against macroscopic preda-  
1736 tors is actually an evolutionary driving force for this  
1737 phenotype.

### 1738 ***Flo11p*-dependent ruffles impact colonial** 1739 **heat dissipation**

1740 Colony ruffling increases the surface-to-volume ratio and may  
1741 provide benefits such as efficient thermoregulation, or other  
1742 such adaptations to the environment (Palková and Váchová  
1743 2006). We also observed that heat-shock response proteins  
1744 were among the most induced surface-growth targets (Figure  
1745 6A, *HSP33* and *SNO4*). To test whether ruffles made by  
1746 *Flo11p*-dependent adhesion impact the temperatures of col-  
1747 onies, ruffled wild-type colonies and smooth *flo11Δ* colonies  
1748 were examined by infrared imaging (Figure 8A). Thermal  
1749

---

1694 borne GFP (PC2560). *C. elegans* transferred into the colony for 45 min before mounting. Merged fluorescent images of head and tail regions of *C.*  
1695 *elegans* showing fluorescent *S. cerevisiae* inside the animal (merged). Fluorescent images of individual *S. cerevisiae* inside the animal (inset = GFP). (G)  
1696 Bar graph showing difference in average number of *S. cerevisiae* cells in the *C. elegans* pharynx between WT and *flo11Δ* colonies. Error bars are SE.  
1697 \*  $P < 0.05$ . WT, wild-type; YEPD, yeast extract, peptone, and dextrose.



1755 imaging showed that the average temperature of a ruffled  
1756 colony was 0.31° Cooler than the average temperature of a  
1757 smooth colony (Figure 8B, black bars,  $P < 0.05$ ,  $n = 6$ ). The  
1758 average coolest region of a ruffled colony was 0.33° Cooler  
1759 than the average coolest region of a smooth colony (Figure  
1760 8B, white bars,  $P < 0.05$ ,  $n = 6$ ). Additionally, the coolest  
1761 regions of the ruffled colonies (Figure 8C,  $<30^\circ$ ) were the  
1762 ruffles themselves (Figure 8C, merged). In a study of cell wall  
1763 stresses, *flo11Δ* cells were also shown to have modest tem-  
1764 perature sensitivity at 37° (Chow *et al.* 2018). In summary,  
1765 Flo11p-dependent ruffling might aid thermoregulation in  
1766 yeast colonies.

## 1767 Discussion

1770 Here, we explored the role of signaling pathways that regulate  
1771 filamentous growth in mediating adhesion-based surface re-  
1772 sponses, including mat formation and colony patterning.  
1773 Fungal cells commonly grow on surfaces, which poses unique  
1774 challenges due to the heterogeneity of the nutrients within  
1775 different parts of the colony and direct exposure to environ-  
1776 mental conditions. Understanding the responses to growth on  
1777 surfaces is important because fungal pathogens exhibit mat  
1778 growth and form invasive filaments (e.g., hyphae) on the  
1779 surface of the host, and on inert surfaces; during early steps  
1780 in host colonization.

### 1781 Analysis of signaling pathways that coregulate 1782 adhesion-dependent surface responses

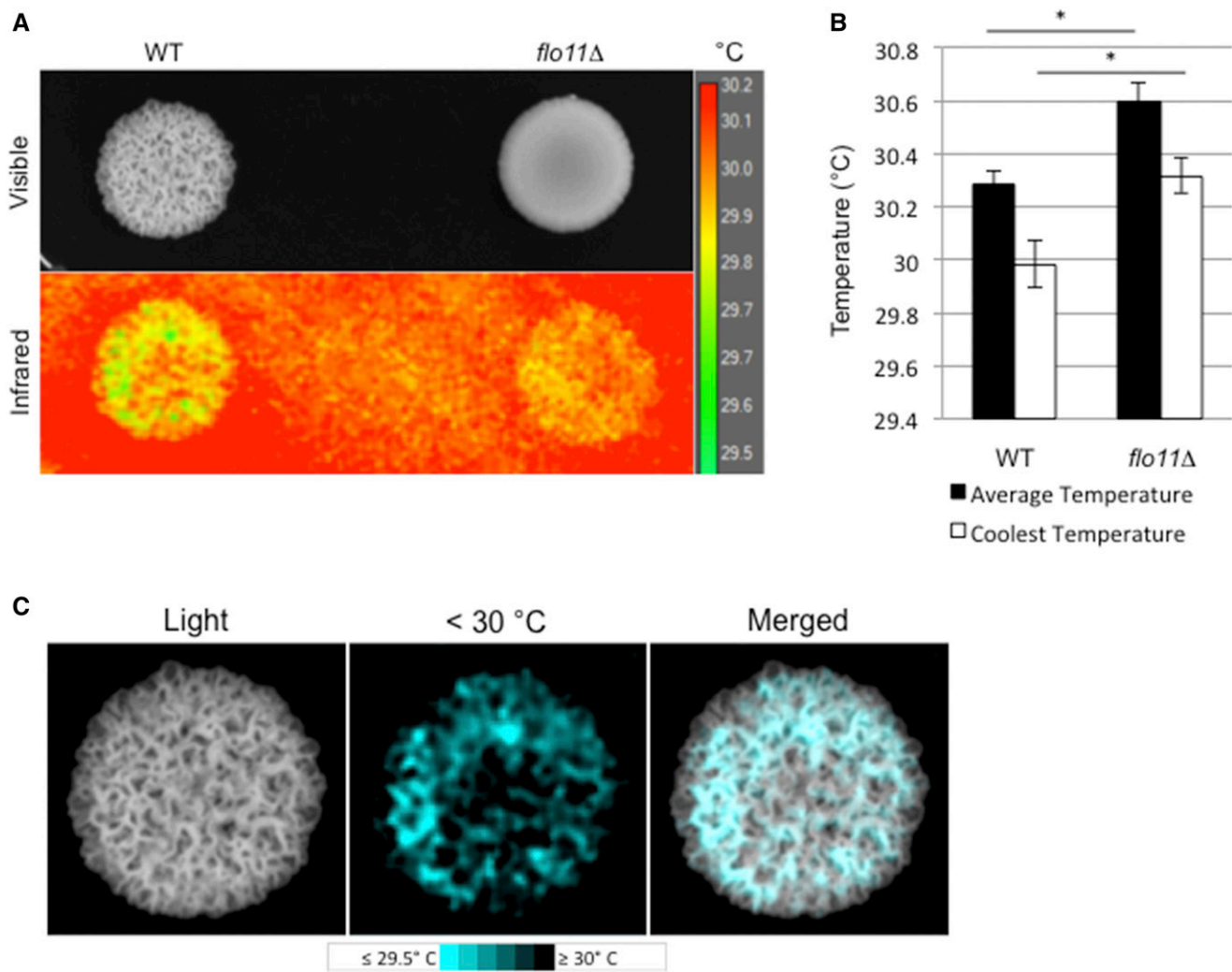
1783 Intracellular signaling pathways can operate in functionally  
1784 interconnected networks (Levchenko 2003). How multiple  
1785 pathways operate in a coordinated manner to achieve mor-  
1786 phogenetic responses with high fidelity remains a mystery. By  
1787 examining the major signaling pathways that regulate fila-  
1788 mentous growth in yeast, we have identified new roles for the  
1789 filamentation network in regulating colony patterning and  
1790 mat growth. Thus, the filamentation regulatory pathways  
1791 may have a general function in regulating the growth of cells  
1792 in surface communities.

1794 We also have identified the chromatin remodeling com-  
1795 plex, SAGA, to be a regulator of filamentous growth. SAGA  
1796 and the previously characterized Rpd3p pathway (Bernstein  
1797 *et al.* 2000; Chavel *et al.* 2010) are involved in the epigenetic  
1798 modification of chromatin. SAGA is an evolutionarily con-  
1799 served chromatin remodeling complex and a member of the  
1800 histone acetyltransferase family of proteins (Wang and Dent  
1801 2014). SAGA's functions are diverse but include changes in  
1802 transcription that result in cell differentiation (Wang and  
1803 Dent 2014; Hirsch *et al.* 2015). In yeast, SAGA controls the  
1804 expression of a specific set of growth-promoting genes  
1805 (Bruzzone *et al.* 2018). In fission yeast, TORC1 and TORC2  
1806 converge to regulate SAGA in response to nutrient availabil-  
1807 ity (Laboucaré *et al.* 2017). Moreover, components of SAGA  
1808 have recently been shown to impact the virulence of  
1809 *Fusarium* (Gao *et al.* 2014).

1811 Expression profiling was performed to evaluate the roles  
1812 for a subset of pathways that regulate adhesion-dependent  
1813 surface growth. We identified an unexpectedly large number  
1814 of differentially expressed genes. Many of the genes were  
1815 regulated by a single pathway. However, as might be expected  
1816 of a dense network of functionally connected pathways, each  
1817 pathway impacted every other pathway by regulating over-  
1818 lapping targets as well as genes encoding pathway compo-  
1819 nents. A key example of this overlap, even in the expanded set  
1820 of pathways, was the gene encoding the adhesion molecule  
1821 Flo11p. This may be expected given the critical roles that  
1822 Flo11p plays in regulating filamentous growth (Rupp *et al.*  
1823 1999), mat formation (Reynolds and Fink 2001), and colo-  
1824 nial patterning (Granek and Magwene 2010). Moreover, the  
1825 *FLO11* gene is a hub where many signaling pathways and  
1826 transcription factors converge (Rupp *et al.* 1999). The other  
1827 gene was *PGU1*, which encodes a secreted plant cell wall-  
1828 degrading enzyme. Given that one surface that budding yeast  
1829 commonly encounter is the surface of plants, especially rot-  
1830 ting fruit, it may not be surprising that yeast induce this gene  
1831 when undergoing surface growth. Transcriptional induction  
1832 of the *PGU1* gene may also result from the growth of cells on  
1833 agar, which is a potential substrate, and may be independ-  
1834 ently regulated. Therefore, one function of the filamenta-  
1835 tion regulatory network may be to coordinately regulate  
1836 target genes that are needed to respond to the challenges  
1837 of growing on surfaces.

1838 We further uncovered new connections between signaling  
1839 pathways that regulate adhesion-dependent surface growth.  
1840 One connection was between the RAS and RTG pathways,  
1841 which coregulated a substantial number of target genes. The  
1842 coregulated targets support a function for the RAS pathway in  
1843 mitochondrial control. The RAS pathway is a global nutrient-  
1844 sensing pathway in yeast and other organisms (Zaman *et al.*  
1845 2008). The fact that RAS coregulates targets of the RTG  
1846 pathway supports the idea that RAS plays a critical role in  
1847 the response to mitochondrial stress. Our results are consis-  
1848 tent with previous observations that connect RAS to the over-  
1849 all regulation of the mitochondria. RAS is required for growth  
1850 on nonfermentable carbon sources, mitochondrial enzyme  
1851 content (Dejean *et al.* 2002), and citrate synthase activity  
1852 (Swiegers *et al.* 2006; Chavel *et al.* 2014). Interestingly, com-  
1853 ponents of the RAS pathway, including the GTPase activating  
1854 protein *Iralp* and adenylate cyclase *Cyr1p*, associate with  
1855 mitochondrial membranes, which might impact RAS path-  
1856 way function or activity at this site (Belotti *et al.* 2012). More-  
1857 over, RAS has been implicated in working with RTG to  
1858 promote longevity in yeast (Kirchman *et al.* 1999). Thus,  
1859 the functional interaction between the two pathways to reg-  
1860 ulate aspects of mitochondrial health might impact the cell's  
1861 overall life span. Further experiments will be required to de-  
1862 termine how the RAS and RTG pathways coordinate the re-  
1863 sponse to mitochondrial problems. Though the nature of this  
1864 relationship is unclear, subsequent studies may better char-  
1865 acterize the mechanism by which each pathway regulates the  
1866 other's hallmark targets.

1867  
1868  
1869  
1870  
1871  
1872  
1873  
1874  
1875  
1876  
1877  
1878  
1879  
1880  
1881  
1882  
1883  
1884  
1885  
1886  
1887  
1888  
1889  
1890  
1891  
1892  
1893  
1894  
1895  
1896  
1897  
1898  
1899  
1900  
1901  
1902  
1903  
1904  
1905  
1906  
1907  
1908  
1909  
1910  
1911  
1912  
1913  
1914  
1915  
1916  
1917  
1918  
1919  
1920  
1921  
1922



1923  
1924  
1925  
1926  
1927  
1928  
1929  
1930  
1931  
1932  
1933  
1934  
1935  
1936  
1937  
1938  
1939  
1940  
1941  
1942  
1943  
1944  
1945  
1946  
1947  
1948  
1949  
1950  
1951  
1952  
1953  
1954  
1955  
1956  
1957  
1958  
1959  
1960  
1961  
1962  
1963  
1964  
1965  
1966  
1967  
1968  
1969  
1970  
1971  
1972  
1973  
1974  
1975  
1976  
1977  
1978

**Figure 8** Effect of cell–cell adhesion on thermoregulation. (A) Visible and infrared images of WT and *flo11Δ* colonies. Colonies were incubated at 30° and removed from the incubator. The image was taken at < 30 sec after removal of lid. Scale temperature in degrees Celsius. (B) Difference in average and coolest recorded temperatures between WT and *flo11Δ*. \*  $P < 0.05$ ,  $n = 6$ . (C) Visible light (Light) and thermal images of cool colony regions (< 30°) of the WT colony from (A). “Merged” shows the overlapping of cool regions with colony ruffles. WT, wild-type.

We also show that *Dig1p* and *Ste12p*, which are commonly thought to reciprocally regulate the same set of target genes, actually regulated a partially nonoverlapping set of targets. One that stood out in the *Dig1p*-regulated set were genes that play a role in zinc uptake and metabolism. This observation is consistent with a previous set of findings that show unique expression profiles and binding sites for this activator–repressor pair (Breitkreutz *et al.* 2003; Zeitlinger *et al.* 2003).

**Yeast respond to surface growth by expressing a subset of stress-response genes**

We also explored the hypothesis that the activity of signaling pathways may change in different parts of a colony over time. We found this to be the case: the activity of the fMAPK pathway was different in different parts of the colony and in different aged colonies. This finding has broad implications in understanding how target genes might be induced during surface growth. For example, it might be expected that other time

points or harvesting from certain regions of the colony might result in different expression profiles. The comparative RNA-seq analysis performed here may be an oversimplification of the actual gene expression changes that occur within a colony, which may vary in different parts of a colony and over time.

In the study, we also examined genes that were differentially expressed during surface growth as compared to growth in liquid culture. The genes that were differentially expressed tell us about the challenges of growing in the unique environment of surface growth. Several of the differentially expressed genes identified fit with what one expects cells to encounter when growing on surfaces. One might expect that cells experience anaerobic stress within colonies compared to when growing in liquid conditions, where they are uniformly aerated by shaking. Likewise, cells in colony exteriors would be expected to be vulnerable to desiccation. Interestingly, we show that colony growth patterns change in response to these

stresses. Specifically, differentially regulated genes impact colony patterning in response to stress.

One prominent class of differentially expressed genes regulates the heat-shock response. This discovery was at first perplexing, given that cells were grown in liquid and on plates at the same temperature. However, thermal imaging verified that colonies do not have a uniform temperature. This may result from the generation of heat due to metabolic activities of cells within the colony, which may lead to temperature differences in different parts of the colony. We also show that ruffles dissipate heat more efficiently than other parts of the colony. The increased surface area of ruffles may promote heat dissipation. Therefore, another function of colony pattern formation might be to efficiently dissipate heat that results from cellular metabolic activities.

### **Adhesive contacts between yeast cells may offer protection from macroscopic predators**

Yeast and other microbes produce colonies that have a ruffled appearance due to contacts between cells. One established reason for cooperation among individuals in microbial populations is protection (West *et al.* 2007). For example, cells in the exterior of flocs protect cells in the interior from toxins and antibiotics (Smukalla *et al.* 2008). Microbial cells are also subject to predation by macroscopic predators. Macroscopic predators, like nematodes, graze on microbial communities. Predator-prey interactions have been studied in bacterial populations, which have developed diverse strategies to evade macroscopic predators. Depending on the species, bacteria have been shown to evade predators by the formation of mats (Darby *et al.* 2002; DePas *et al.* 2014; Nandi *et al.* 2016), by the secretion of proteases (Vaitkevicius *et al.* 2006) and exopolysaccharides that interfere with the predator's responses (Begun *et al.* 2007), and by phase variation, in which bacterial cells express different classes of cell surface proteins to evade detection (Dahl *et al.* 2011).

Although predator-prey studies are less-well characterized in fungal species, yeast and other fungal microorganisms have ecologically relevant interactions with animals in the wild, including grazing by wasps (Stefanini *et al.* 2016), flies (Fischer *et al.* 2017), and other invertebrates. Using two well-characterized laboratory genetic models, we provide evidence that adhesive contacts between yeast cells may deter efficient predation by nematodes. While individual cells in suspension were vulnerable to being ingested, cells that adhered to each other and formed clumps were too large to be eaten. Once cells settled out of suspension and grew into a colony, adhesive colonies formed a physical barrier to deter penetration by worms and also trigger the "nose-touch" mechanosensory behavioral avoidance response. Although the predator-prey model set up in the laboratory may or may not reflect a true ecological relationship between the two species, experiments using model organisms can provide insights into encounters that may occur in the wild. Our data provide an empirical framework to test the hypothesis that

the physical interaction among yeast cells in communities can protect individuals from macroscopic predation in the wild.

In conclusion, we have explored the roles of filamentous growth regulatory pathways in regulating multiple adhesion-dependent surface responses in yeast. Dissection of the regulatory pathways by comparative RNA-seq and mutant phenotype analysis revealed new components and targets, which emphasize the common and unique roles that pathways play in coordinately regulating colonial surface responses in this organism. Stress-responsive genes that respond to challenges associated with surface growth were also characterized. The signaling components, target genes, and stress-responsive genes identified here might be common among other fungi, including pathogens. Our results may extend specifically to early steps in fungal virulence, where cells must attach to and penetrate surfaces to colonize the host.

### **Acknowledgments**

Clark Driscoll and Aditi Chaubey helped with experiments involving *C. elegans*. Thank you to laboratory members for comments on the article. The work was supported by grants from the National Institutes of Health (GM-098629 to P.J.C. and GM-015758 to D.M.F.).

Author contributions: J.C. designed and performed experiments and wrote the paper. I.S. analyzed the data. S.-J. performed experiments and analyzed the data. O.M. performed experiments. O.G. analyzed the data. D.M.F. designed experiments. A.K. analyzed the data. P.J.C. designed experiments and wrote the paper. The authors have no competing interests in the study.

### **Literature Cited**

- Abdullah, U., and P. J. Cullen, 2009 The tRNA modification complex elongator regulates the Cdc42-dependent mitogen-activated protein kinase pathway that controls filamentous growth in yeast. *Eukaryot. Cell* 8: 1362–1372. <https://doi.org/10.1128/EC.00015-09>
- Adhikari, H., and P. J. Cullen, 2014 Metabolic respiration induces AMPK- and Ire1p-dependent activation of the p38-type HOG MAPK pathway. *PLoS Genet.* 10: e1004734. <https://doi.org/10.1371/journal.pgen.1004734>
- Anders, S., P. T. Pyl, and W. Huber, 2015 HTSeq—a Python framework to work with high-throughput sequencing data. *Bioinformatics* 31: 166–169. <https://doi.org/10.1093/bioinformatics/btu638>
- Ashburner, M., C. A. Ball, J. A. Blake, D. Botstein, H. Butler *et al.*, 2000 Gene ontology: tool for the unification of biology. The gene ontology consortium. *Nat. Genet.* 25: 25–29. <https://doi.org/10.1038/75556>
- Avery, L., and B. B. Shtonda, 2003 Food transport in the *C. elegans* pharynx. *J. Exp. Biol.* 206: 2441–2457. <https://doi.org/10.1242/jeb.00433>
- Bardwell, L., J. G. Cook, J. X. Zhu-Shimoni, D. Voora, and J. Thorner, 1998 Differential regulation of transcription: repression by unactivated mitogen-activated protein kinase Kss1 requires the Dig1 and Dig2 proteins. *Proc. Natl. Acad. Sci. USA* 95: 15400–15405. <https://doi.org/10.1073/pnas.95.26.15400>

- 2091 Barrales, R. R., J. Jimenez, and J. I. Ibeas, 2008 Identification of  
2092 novel activation mechanisms for FLO11 regulation in *Saccharo-*  
2093 *myces cerevisiae*. *Genetics* 178: 145–156. [https://doi.org/](https://doi.org/10.1534/genetics.107.081315)  
2094 [10.1534/genetics.107.081315](https://doi.org/10.1534/genetics.107.081315)
- 2095 Basehoar, A. D., S. J. Zanton, and B. F. Pugh, 2004 Identification  
2096 and distinct regulation of yeast TATA box-containing genes. *Cell*  
2097 116: 699–709. [https://doi.org/10.1016/S0092-](https://doi.org/10.1016/S0092-8674(04)00205-3)  
2098 [8674\(04\)00205-3](https://doi.org/10.1016/S0092-8674(04)00205-3)
- 2099 Begun, J., J. M. Gaiani, H. Rohde, D. Mack, S. B. Calderwood *et al.*,  
2100 2007 Staphylococcal biofilm exopolysaccharide protects  
2101 against *Caenorhabditis elegans* immune defenses. *PLoS Pathog.*  
2102 3: e57. <https://doi.org/10.1371/journal.ppat.0030057>
- 2103 Belotti, F., R. Tisi, C. Paiardi, M. Rigamonti, S. Groppi *et al.*,  
2104 2012 Localization of Ras signaling complex in budding yeast.  
2105 *Biochim. Biophys. Acta* 1823: 1208–1216. [https://doi.org/](https://doi.org/10.1016/j.bbamcr.2012.04.016)  
2106 [10.1016/j.bbamcr.2012.04.016](https://doi.org/10.1016/j.bbamcr.2012.04.016)
- 2107 Bentley, N. J., I. T. Fitch, and M. F. Tuite, 1992 The small heat-  
2108 shock protein Hsp26 of *Saccharomyces cerevisiae* assembles in-  
2109 to a high molecular weight aggregate. *Yeast* 8: 95–106. <https://doi.org/10.1002/yea.320080204>
- 2110 Bernstein, B. E., J. K. Tong, and S. L. Schreiber, 2000  
2111 Genomewide studies of histone deacetylase function in  
2112 yeast. *Proc. Natl. Acad. Sci. USA* 97: 13708–13713 [corrigenda:  
2113 *Proc. Natl. Acad. Sci. USA* 98: 5368 (2001)]. [https://doi.org/](https://doi.org/10.1073/pnas.250477697)  
2114 [10.1073/pnas.250477697](https://doi.org/10.1073/pnas.250477697)
- 2115 Bharucha, N., J. Ma, C. J. Dobry, S. K. Lawson, Z. Yang *et al.*,  
2116 2008 Analysis of the yeast kinome reveals a network of regu-  
2117 lated protein localization during filamentous growth. *Mol. Biol.*  
2118 *Cell* 19: 2708–2717. [https://doi.org/10.1091/mbc.e07-11-](https://doi.org/10.1091/mbc.e07-11-1199)  
2119 [1199](https://doi.org/10.1091/mbc.e07-11-1199)
- 2120 Bois, M., S. Singh, A. Samlalsingh, P. N. Lipke, and M. C. Garcia,  
2121 2013 Does *Candida albicans* Als5p amyloid play a role in com-  
2122 mensalism in *Caenorhabditis elegans*? *Eukaryot. Cell* 12: 703–  
2123 711. <https://doi.org/10.1128/EC.00020-13>
- 2124 Bojsen, R. K., K. S. Andersen, and B. Regenberg, 2012  
2125 *Saccharomyces cerevisiae*—a model to uncover molecular  
2126 mechanisms for yeast biofilm biology. *FEMS Immunol. Med.*  
2127 *Microbiol.* 65: 169–182. [https://doi.org/10.1111/j.1574-](https://doi.org/10.1111/j.1574-695X.2012.00943.x)  
2128 [695X.2012.00943.x](https://doi.org/10.1111/j.1574-695X.2012.00943.x)
- 2129 Bojsen, R., B. Regenberg, D. Gresham, and A. Folkesson, 2016 A  
2130 common mechanism involving the TORC1 pathway can lead to  
2131 amphotericin B-persistence in biofilm and planktonic *Saccharo-*  
2132 *myces cerevisiae* populations. *Sci. Rep.* 6: 21874. <https://doi.org/10.1038/srep21874>
- 2133 Borneman, A. R., J. A. Leigh-Bell, H. Yu, P. Bertone, M. Gerstein  
2134 *et al.*, 2006 Target hub proteins serve as master regulators of  
2135 development in yeast. *Genes Dev.* 20: 435–448. [https://doi.org/](https://doi.org/10.1101/gad.1389306)  
2136 [10.1101/gad.1389306](https://doi.org/10.1101/gad.1389306)
- 2137 Breikreutz, A., L. Boucher, B. J. Breikreutz, M. Sultan, I. Jurisica  
2138 *et al.*, 2003 Phenotypic and transcriptional plasticity directed  
2139 by a yeast mitogen-activated protein kinase network. *Genetics*  
2140 165: 997–1015.
- 2141 Brenner, S., 1974 The genetics of *Caenorhabditis elegans*. *Genet-*  
2142 *ics* 77: 71–94.
- 2143 Bruzzone, M. J., S. Grunberg, S. Kubik, G. E. Zentner, and D. Shore,  
2144 2018 Distinct patterns of histone acetyltransferase and Medi-  
2145 ator deployment at yeast protein-coding genes. *Genes Dev.* 32:  
2146 1252–1265. <https://doi.org/10.1101/gad.312173.118>
- 2147 Chan, C. X., S. El-Kirat-Chatel, I. G. Joseph, D. N. Jackson, C. B.  
2148 Ramscook *et al.*, 2016 Force sensitivity in *Saccharomyces cer-*  
2149 *visiae* flocculins. *mSphere* 1: e00128-16. [https://doi.org/](https://doi.org/10.1128/mSphere.00128-16)  
2150 [10.1128/mSphere.00128-16](https://doi.org/10.1128/mSphere.00128-16)
- 2151 Chandra, J., D. M. Kuhn, P. K. Mukherjee, L. L. Hoyer, T. McCor-  
2152 mick *et al.*, 2001 Biofilm formation by the fungal pathogen  
2153 *Candida albicans*: development, architecture, and drug resis-  
2154 tance. *J. Bacteriol.* 183: 5385–5394. [https://doi.org/10.1128/](https://doi.org/10.1128/JB.183.18.5385-5394.2001)  
2155 [JB.183.18.5385-5394.2001](https://doi.org/10.1128/JB.183.18.5385-5394.2001)
- 2156 Chavel, C. A., H. M. Dionne, B. Birkaya, J. Joshi, and P. J. Cullen,  
2157 2010 Multiple signals converge on a differentiation MAPK  
2158 pathway. *PLoS Genet.* 6: e1000883. [https://doi.org/10.1371/](https://doi.org/10.1371/journal.pgen.1000883)  
2159 [journal.pgen.1000883](https://doi.org/10.1371/journal.pgen.1000883)
- 2160 Chavel, C. A., L. M. Caccamise, B. Li, and P. J. Cullen, 2014  
2161 Global regulation of a differentiation MAPK pathway in yeast. *Genetics*  
2162 198: 1309–1328. [https://doi.org/10.1534/genet-](https://doi.org/10.1534/genetics.114.168252)  
2163 [ics.114.168252](https://doi.org/10.1534/genetics.114.168252)
- 2164 Chin, B. L., O. Ryan, F. Lewitter, C. Boone, and G. R. Fink,  
2165 2012 Genetic variation in *Saccharomyces cerevisiae*: circuit  
2166 diversification in a signal transduction network. *Genetics* 192:  
2167 1523–1532. <https://doi.org/10.1534/genetics.112.145573>
- 2168 Chou, S., S. Lane, and H. Liu, 2006 Regulation of mating and  
2169 filamentation genes by two distinct Ste12 complexes in *Saccha-*  
2170 *romyces cerevisiae*. *Mol. Cell. Biol.* 26: 4794–4805. <https://doi.org/10.1128/MCB.02053-05>
- 2171 Chow, J., M. Notaro, A. Prabhakar, S. J. Free, and P. J. Cullen,  
2172 2018 Impact of fungal MAPK pathway targets on the cell wall.  
2173 *J. Fungi (Basel)* 4: E93. <https://doi.org/10.3390/jof4030093>
- 2174 Chow, J., H. M. Dionne, A. Prabhakar, A. Mehrotra, J. Sombon-  
2175 thum *et al.*, 2019 Aggregate filamentous growth responses in  
2176 yeast. *mSphere* 4: e00702-18. [https://doi.org/10.1128/](https://doi.org/10.1128/mSphere.00702-18)  
2177 [mSphere.00702-18](https://doi.org/10.1128/mSphere.00702-18)
- 2178 Cohen, B. D., O. Sertil, N. E. Abramova, K. J. Davies, and C. V.  
2179 Lowry, 2001 Induction and repression of DAN1 and the family  
2180 of anaerobic mannoprotein genes in *Saccharomyces cerevisiae*  
2181 occurs through a complex array of regulatory sites. *Nucleic*  
2182 *Acids Res.* 29: 799–808. <https://doi.org/10.1093/nar/29.3.799>
- 2183 Coluccio, A., E. Bogengruber, M. N. Conrad, M. E. Dresser, P. Briza  
2184 *et al.*, 2004 Morphogenetic pathway of spore wall assembly in  
2185 *Saccharomyces cerevisiae*. *Eukaryot. Cell* 3: 1464–1475.  
2186 <https://doi.org/10.1128/EC.3.6.1464-1475.2004>
- 2187 Cook, J. G., L. Bardwell, S. J. Kron, and J. Thorner, 1996 Two  
2188 novel targets of the MAP kinase Kss1 are negative regulators of  
2189 invasive growth in the yeast *Saccharomyces cerevisiae*. *Genes*  
2190 *Dev.* 10: 2831–2848. <https://doi.org/10.1101/gad.10.22.2831>
- 2191 Crabtree, H. G., 1929 Observations on the carbohydrate metabo-  
2192 lism of tumours. *Biochem. J.* 23: 536–545. [https://doi.org/](https://doi.org/10.1042/bj0230536)  
2193 [10.1042/bj0230536](https://doi.org/10.1042/bj0230536)
- 2194 Cromie, G. A., Z. Tan, M. Hays, A. Sirt, E. W. Jeffery *et al.*,  
2195 2017 Transcriptional profiling of biofilm regulators identified  
2196 by an overexpression screen in *Saccharomyces cerevisiae*. *G3*  
2197 (Bethesda) 7: 2845–2854. [https://doi.org/10.1534/](https://doi.org/10.1534/g3.117.042440)  
2198 [g3.117.042440](https://doi.org/10.1534/g3.117.042440)
- 2199 Cullen, P. J., 2015a Evaluating the activity of the filamentous  
2200 growth mitogen-activated protein kinase pathway in yeast. *Cold*  
2201 *Spring Harb. Protoc.* 2015: 276–283. [https://doi.org/10.1101/](https://doi.org/10.1101/pdb.prot085092)  
2202 [pdb.prot085092](https://doi.org/10.1101/pdb.prot085092)
- 2203 Cullen, P. J., 2015b The plate-washing assay: a simple test for  
2204 filamentous growth in budding yeast. *Cold Spring Harb. Protoc.*  
2205 2015: 168–171. <https://doi.org/10.1101/pdb.prot085068>
- 2206 Cullen, P. J., and G. F. Sprague, Jr., 2000 Glucose depletion  
2207 causes haploid invasive growth in yeast. *Proc. Natl. Acad. Sci.*  
2208 *USA* 97: 13619–13624. [https://doi.org/10.1073/](https://doi.org/10.1073/pnas.240345197)  
2209 [pnas.240345197](https://doi.org/10.1073/pnas.240345197)
- 2210 Cullen, P. J., and G. F. Sprague, Jr., 2002 The roles of bud-site-  
2211 selection proteins during haploid invasive growth in yeast. *Mol.*  
2212 *Biol. Cell* 13: 2990–3004. [https://doi.org/10.1091/mbc.e02-](https://doi.org/10.1091/mbc.e02-03-0151)  
2213 [03-0151](https://doi.org/10.1091/mbc.e02-03-0151)
- 2214 Cullen, P. J., and G. F. Sprague, Jr., 2012 The regulation of fila-  
2215 mentous growth in yeast. *Genetics* 190: 23–49. [https://doi.org/](https://doi.org/10.1534/genetics.111.127456)  
2216 [10.1534/genetics.111.127456](https://doi.org/10.1534/genetics.111.127456)
- 2217 Cullen, P. J., W. Sabbagh, Jr., E. Graham, M. M. Irick, E. K. van  
2218 Olden *et al.*, 2004 A signaling mucin at the head of the Cdc42-  
2219 and MAPK-dependent filamentous growth pathway in yeast.  
2220 *Genes Dev.* 18: 1695–1708. [https://doi.org/10.1101/](https://doi.org/10.1101/gad.1178604)  
2221 [gad.1178604](https://doi.org/10.1101/gad.1178604)

- 2203 Cutler, N. S., X. Pan, J. Heitman, and M. E. Cardenas, 2001 The  
2204 TOR signal transduction cascade controls cellular differentiation  
2205 in response to nutrients. *Mol. Biol. Cell* 12: 4103–4113. <https://doi.org/10.1091/mbc.12.12.4103>
- 2206 Dahl, J. L., C. H. Ulrich, and T. L. Kroft, 2011 Role of phase  
2207 variation in the resistance of *Myxococcus xanthus* fruiting bod-  
2208 ies to *Caenorhabditis elegans* predation. *J. Bacteriol.* 193: 5081–  
2209 5089. <https://doi.org/10.1128/JB.05383-11>
- 2210 Dang, N. X., and D. K. Hinch, 2011 Identification of two hydro-  
2211 philins that contribute to the desiccation and freezing tolerance  
2212 of yeast (*Saccharomyces cerevisiae*) cells. *Cryobiology* 62: 188–  
2213 193. <https://doi.org/10.1016/j.cryobiol.2011.03.002>
- 2214 Darby, C., J. W. Hsu, N. Ghori, and S. Falkow,  
2002 *Caenorhabditis elegans*: plague bacteria biofilm blocks  
2215 food intake. *Nature* 417: 243–244. <https://doi.org/10.1038/417243a>
- 2216 De Deken, R. H., 1966 The Crabtree effects and its relation to the  
2217 petite mutation. *J. Gen. Microbiol.* 44: 157–165. <https://doi.org/10.1099/00221287-44-2-157>
- 2218 Dejean, L., B. Beauvoit, O. Bunoust, B. Guerin, and M. Rigoulet,  
2002 Activation of Ras cascade increases the mitochondrial  
2219 enzyme content of respiratory competent yeast. *Biochem. Biophys. Res. Commun.* 293: 1383–1388. [https://doi.org/10.1016/S0006-291X\(02\)00391-1](https://doi.org/10.1016/S0006-291X(02)00391-1)
- 2220 DePas, W. H., A. K. Syed, M. Sifuentes, J. S. Lee, D. Warshaw *et al.*,  
2014 Biofilm formation protects *Escherichia coli* against killing  
2221 by *Caenorhabditis elegans* and *Myxococcus xanthus*. *Appl. Environ. Microbiol.* 80: 7079–7087. <https://doi.org/10.1128/AEM.02464-14>
- 2222 Desai, J. V., A. P. Mitchell, and D. R. Andes, 2014 Fungal biofilms,  
2223 drug resistance, and recurrent infection. *Cold Spring Harb. Perspect. Med.* 4: a019729. <https://doi.org/10.1101/cshperspect.a019729>
- 2224 Dowell, R. D., O. Ryan, A. Jansen, D. Cheung, S. Agarwala *et al.*,  
2010 Genotype to phenotype: a complex problem. *Science* 328: 469. <https://doi.org/10.1126/science.1189015>
- 2225 Eden, E., D. Lipson, S. Yogev, and Z. Yakhini, 2007 Discovering  
2226 motifs in ranked lists of DNA sequences. *PLoS Comput. Biol.* 3: e39. <https://doi.org/10.1371/journal.pcbi.0030039>
- 2227 Eden, E., R. Navon, I. Steinfeld, D. Lipson, and Z. Yakhini,  
2009 GOrilla: a tool for discovery and visualization of enriched  
2228 GO terms in ranked gene lists. *BMC Bioinformatics* 10: 48. <https://doi.org/10.1186/1471-2105-10-48>
- 2229 Engebrecht, J., S. Masse, L. Davis, K. Rose, and T. Kessel,  
1998 Yeast meiotic mutants proficient for the induction of  
2230 ectopic recombination. *Genetics* 148: 581–598.
- 2231 Epstein, C. B., J. A. Waddle, W. Hale, V. Dave, J. Thornton *et al.*,  
2001 Genome-wide responses to mitochondrial dysfunction. *Mol. Biol. Cell* 12: 297–308. <https://doi.org/10.1091/mbc.12.2.297>
- 2232 Fang-Yen, C., L. Avery, and A. D. Samuel, 2009 Two size-selective  
2233 mechanisms specifically trap bacteria-sized food particles in  
2234 *Caenorhabditis elegans*. *Proc. Natl. Acad. Sci. USA* 106: 20093–20096. <https://doi.org/10.1073/pnas.0904036106>
- 2235 Félix, M. A., and C. Braendle, 2010 The natural history of *Caenorhabditis elegans*. *Curr. Biol.* 20: R965–R969. <https://doi.org/10.1016/j.cub.2010.09.050>
- 2236 Fischer, C. N., E. P. Trautman, J. M. Crawford, E. V. Stabb, J. Handelsman *et al.*, 2017 Metabolite exchange between microbiome members produces compounds that influence *Drosophila* behavior. *Elife* 6: e18855. <https://doi.org/10.7554/eLife.18855>
- 2237 Gao, T., Z. Zheng, Y. Hou, and M. Zhou, 2014 Transcription factors spt3 and spt8 are associated with conidiation, mycelium growth, and pathogenicity in *Fusarium graminearum*. *FEMS Microbiol. Lett.* 351: 42–50. <https://doi.org/10.1111/1574-6968.12350>
- 2238 Garay-Arroyo, A., and A. A. Covarrubias, 1999 Three genes whose  
2239 expression is induced by stress in *Saccharomyces cerevisiae*.  
2240 *Yeast* 15: 879–892. [https://doi.org/10.1002/\(SICI\)1097-0061\(199907\)15:10A<879::AID-YEA428>3.0.CO;2-Q](https://doi.org/10.1002/(SICI)1097-0061(199907)15:10A<879::AID-YEA428>3.0.CO;2-Q)
- 2241 Georgakopoulos, T., and G. Thireos, 1992 Two distinct yeast tran-  
2242 scriptional activators require the function of the GCN5 protein  
2243 to promote normal levels of transcription. *EMBO J.* 11: 4145–  
2244 4152. <https://doi.org/10.1002/j.1460-2075.1992.tb05507.x>
- 2245 Gietz, R. D., and R. H. Schiest, 2007 High-efficiency yeast trans-  
2246 formation using the LiAc/SS carrier DNA/PEG method. *Nat. Protoc.* 2: 31–34. <https://doi.org/10.1038/nprot.2007.13>
- 2247 Gimeno, C. J., P. O. Ljungdahl, C. A. Styles, and G. R. Fink,  
1992 Unipolar cell divisions in the yeast *S. cerevisiae* lead to  
2248 filamentous growth: regulation by starvation and RAS. *Cell* 68: 1077–1090. [https://doi.org/10.1016/0092-8674\(92\)90079-R](https://doi.org/10.1016/0092-8674(92)90079-R)
- 2249 González, B., A. Mas, G. Beltran, P. J. Cullen, and M. J. Torija,  
2017 Role of mitochondrial retrograde pathway in regulating  
2250 ethanol-inducible filamentous growth in yeast. *Front. Physiol.* 8: 148. <https://doi.org/10.3389/fphys.2017.00148>
- 2251 Granek, J. A., and P. M. Magwene, 2010 Environmental and genetic  
2252 determinants of colony morphology in yeast. *PLoS Genet.* 6: e1000823. <https://doi.org/10.1371/journal.pgen.1000823>
- 2253 Granek, J. A., O. Kayikci, and P. M. Magwene, 2011 Pleiotropic  
2254 signaling pathways orchestrate yeast development. *Curr. Opin. Microbiol.* 14: 676–681. <https://doi.org/10.1016/j.mib.2011.09.004>
- 2255 Graybill, E. R., M. F. Rouhier, C. E. Kirby, and J. W. Hawes,  
2007 Functional comparison of citrate synthase isoforms from  
2256 *S. cerevisiae*. *Arch. Biochem. Biophys.* 465: 26–37. <https://doi.org/10.1016/j.abb.2007.04.039>
- 2257 Hagman, A., T. Sall, and J. Piskur, 2014 Analysis of the yeast  
2258 short-term Crabtree effect and its origin. *FEBS J.* 281: 4805–  
2259 4814. <https://doi.org/10.1111/febs.13019>
- 2260 Hart, A. C., S. Sims, and J. M. Kaplan, 1995 Synaptic code for  
2261 sensory modalities revealed by *C. elegans* GLR-1 glutamate receptor. *Nature* 378: 82–85. <https://doi.org/10.1038/378082a0>
- 2262 Higgins, V. J., P. J. Rogers, and I. W. Dawes, 2003 Application of  
2263 genome-wide expression analysis to identify molecular markers  
2264 useful in monitoring industrial fermentations. *Appl. Environ. Microbiol.* 69: 7535–7540. <https://doi.org/10.1128/AEM.69.12.7535-7540.2003>
- 2265 Hirsch, C. L., Z. Coban Akdemir, L. Wang, G. Jayakumaran, D. Trcka  
2266 *et al.*, 2015 Myc and SAGA rewire an alternative splicing network during early somatic cell reprogramming. *Genes Dev.* 29: 803–816. <https://doi.org/10.1101/gad.255109.114>
- 2267 Huisinga, K. L., and B. F. Pugh, 2004 A genome-wide housekeeping  
2268 role for TFIID and a highly regulated stress-related role for  
2269 SAGA in *Saccharomyces cerevisiae*. *Mol. Cell* 13: 573–585. [https://doi.org/10.1016/S1097-2765\(04\)00087-5](https://doi.org/10.1016/S1097-2765(04)00087-5)
- 2270 Ignatiadis, N., B. Klaus, J. B. Zaugg, and W. Huber, 2016 Data-driven hypothesis weighting increases detection power in genome-scale multiple testing. *Nat. Methods* 13: 577–580. <https://doi.org/10.1038/nmeth.3885>
- 2271 Jain, C., M. Yun, S. M. Politz, and R. P. Rao, 2009 A pathogenesis  
2272 assay using *Saccharomyces cerevisiae* and *Caenorhabditis elegans* reveals novel roles for yeast AP-1, Yap1, and host dual oxidase BLI-3 in fungal pathogenesis. *Eukaryot. Cell* 8: 1218–1227. <https://doi.org/10.1128/EC.00367-08>
- 2273 James, P., J. Halladay, and E. A. Craig, 1996 Genomic libraries and a host strain designed for highly efficient two-hybrid selection in yeast. *Genetics* 144: 1425–1436.
- 2274 Jin, R., C. J. Dobry, P. J. McCown, and A. Kumar, 2008 Large-scale analysis of yeast filamentous growth by systematic gene disruption and overexpression. *Mol. Biol. Cell* 19: 284–296. <https://doi.org/10.1091/mbc.e07-05-0519>
- 2275 Jones, R. C., and J. S. Hough, 1970 The effect of temperature on the metabolism of baker's yeast growing on continuous culture.

- 2315 J. Gen. Microbiol. 60: 107–116. <https://doi.org/10.1099/00221287-60-1-107>
- 2316
- 2317 Kaksonen, M., Y. Sun, and D. G. Drubin, 2003 A pathway for
- 2318 association of receptors, adaptors, and actin during endocytic
- 2319 internalization. *Cell* 115: 475–487. [https://doi.org/10.1016/S0092-8674\(03\)00883-3](https://doi.org/10.1016/S0092-8674(03)00883-3)
- 2320 Kanehisa, M., and S. Goto, 2000 KEGG: Kyoto Encyclopedia of
- 2321 Genes and Genomes. *Nucleic Acids Res.* 28: 27–30. <https://doi.org/10.1093/nar/28.1.27>
- 2322 Kaplan, J. M., and H. R. Horvitz, 1993 A dual mechanosensory
- 2323 and chemosensory neuron in *Caenorhabditis elegans*. *Proc.*
- 2324 *Natl. Acad. Sci. USA* 90: 2227–2231. <https://doi.org/10.1073/pnas.90.6.2227>
- 2325 Karunanithi, S., N. Vadaie, C. A. Chavel, B. Birkaya, J. Joshi *et al.*,
- 2326 2010 Shedding of the mucin-like flocculin Flo11p reveals a
- 2327 new aspect of fungal adhesion regulation. *Curr. Biol.* 20:
- 2328 1389–1395. <https://doi.org/10.1016/j.cub.2010.06.033>
- 2329 Karunanithi, S., J. Joshi, C. Chavel, B. Birkaya, L. Grell *et al.*,
- 2330 2012 Regulation of mat responses by a differentiation MAPK
- 2331 pathway in *Saccharomyces cerevisiae*. *PLoS One* 7: e32294.
- 2332 <https://doi.org/10.1371/journal.pone.0032294>
- 2333 Kim, J. M., S. Vanguri, J. D. Boeke, A. Gabriel, and D. F. Voytas,
- 2334 1998 Transposable elements and genome organization: a
- 2335 comprehensive survey of retrotransposons revealed by the com-
- 2336 plete *Saccharomyces cerevisiae* genome sequence. *Genome Res.*
- 2337 8: 464–478. <https://doi.org/10.1101/gr.8.5.464>
- 2338 Kim, K. S., M. S. Rosenkrantz, and L. Guarente,
- 2339 1986 *Saccharomyces cerevisiae* contains two functional citrate
- 2340 synthase genes. *Mol. Cell. Biol.* 6: 1936–1942. <https://doi.org/10.1128/MCB.6.6.1936>
- 2341 Kirchman, P. A., S. Kim, C. Y. Lai, and S. M. Jazwinski,
- 2342 1999 Interorganelle signaling is a determinant of longevity
- 2343 in *Saccharomyces cerevisiae*. *Genetics* 152: 179–190.
- 2344 Koutelou, E., C. L. Hirsch, and S. Y. Dent, 2010 Multiple faces of
- 2345 the SAGA complex. *Curr. Opin. Cell Biol.* 22: 374–382. <https://doi.org/10.1016/j.ceb.2010.03.005>
- 2346 Kraushaar, T., S. Bruckner, M. Veelders, D. Rhinow, F. Schreiner
- 2347 *et al.*, 2015 Interactions by the fungal Flo11 adhesin depend
- 2348 on a fibronectin type III-like adhesin domain girdled by aromatic
- 2349 bands. *Structure* 23: 1005–1017. <https://doi.org/10.1016/j.str.2015.03.021>
- 2350 Kuchin, S., V. K. Vyas, and M. Carlson, 2002 Snf1 protein kinase
- 2351 and the repressors Nrg1 and Nrg2 regulate FLO11, haploid in-
- 2352 vasive growth, and diploid pseudohyphal differentiation. *Mol.*
- 2353 *Cell. Biol.* 22: 3994–4000. <https://doi.org/10.1128/MCB.22.12.3994-4000.2002>
- 2354 Kumamoto, C. A., 2005 A contact-activated kinase signals *Candi-*
- 2355 *da albicans* invasive growth and biofilm development. *Proc.*
- 2356 *Natl. Acad. Sci. USA* 102: 5576–5581. <https://doi.org/10.1073/pnas.0407097102>
- 2357 Kusari, A. B., D. M. Molina, W. Sabbagh, Jr., C. S. Lau, and L.
- 2358 Bardwell, 2004 A conserved protein interaction network in-
- 2359 volving the yeast MAP kinases Fus3 and Kss1. *J. Cell Biol.*
- 2360 164: 267–277. <https://doi.org/10.1083/jcb.200310021>
- 2361 Laboucarié, T., D. Detilleux, R. A. Rodriguez-Mias, C. Faux, Y. Ro-
- 2362 meo *et al.*, 2017 TORC1 and TORC2 converge to regulate the
- 2363 SAGA co-activator in response to nutrient availability. *EMBO*
- 2364 *Rep.* 18: 2197–2218. <https://doi.org/10.15252/embr.201744942>
- 2365 Levchenko, A., 2003 Dynamical and integrative cell signaling:
- 2366 challenges for the new biology. *Biotechnol. Bioeng.* 84: 773–
- 2367 782. <https://doi.org/10.1002/bit.10854>
- 2368 Li, W., and A. P. Mitchell, 1997 Proteolytic activation of Rim1p, a
- 2369 positive regulator of yeast sporulation and invasive growth. *Ge-*
- 2370 *netics* 145: 63–73.
- 2371 Liao, X., and R. A. Butow, 1993 RTG1 and RTG2: two yeast genes
- 2372 required for a novel path of communication from mitochondria
- 2373 to the nucleus. *Cell* 72: 61–71. [https://doi.org/10.1016/0092-8674\(93\)90050-Z](https://doi.org/10.1016/0092-8674(93)90050-Z)
- 2374 Lin, D., X. Yin, X. Wang, P. Zhou, and F. B. Guo, 2013 Re-anno-
- 2375 tation of protein-coding genes in the genome of *saccharomyces*
- 2376 *cerevisiae* based on support vector machines. *PLoS One* 8:
- 2377 e64477. <https://doi.org/10.1371/journal.pone.0064477>
- 2378 Liu, H., C. A. Styles, and G. R. Fink, 1993 Elements of the yeast
- 2379 pheromone response pathway required for filamentous growth
- 2380 of diploids. *Science* 262: 1741–1744. <https://doi.org/10.1126/science.8259520>
- 2381 Liu, H., C. A. Styles, and G. R. Fink, 1996 *Saccharomyces cerevi-*
- 2382 *siae* S288C has a mutation in FLO8, a gene required for filamen-
- 2383 tous growth. *Genetics* 144: 967–978.
- 2384 Liu, Z., and R. A. Butow, 1999 A transcriptional switch in the
- 2385 expression of yeast tricarboxylic acid cycle genes in response
- 2386 to a reduction or loss of respiratory function. *Mol. Cell. Biol.*
- 2387 19: 6720–6728. <https://doi.org/10.1128/MCB.19.10.6720>
- 2388 Liu, Z., and R. A. Butow, 2006 Mitochondrial retrograde signal-
- 2389 ing. *Annu. Rev. Genet.* 40: 159–185. <https://doi.org/10.1146/annurev.genet.40.110405.090613>
- 2390 Livak, K. J., and T. D. Schmittgen, 2001 Analysis of relative gene
- 2391 expression data using real-time quantitative PCR and the 2(-
- 2392 Delta Delta C(T)). *Method. Methods* 25: 402–408. <https://doi.org/10.1006/meth.2001.1262>
- 2393 Lo, H. J., J. R. Kohler, B. DiDomenico, D. Loebenberg, A. Caccia-
- 2394 puoti *et al.*, 1997 Nonfilamentous *C. albicans* mutants are avir-
- 2395 ulent. *Cell* 90: 939–949. [https://doi.org/10.1016/S0092-8674\(00\)80358-X](https://doi.org/10.1016/S0092-8674(00)80358-X)
- 2396 Lo, W. S., and A. M. Dranginis, 1998 The cell surface flocculin
- 2397 Flo11 is required for pseudohyphae formation and invasion by
- 2398 *Saccharomyces cerevisiae*. *Mol. Biol. Cell* 9: 161–171. <https://doi.org/10.1091/mbc.9.1.161>
- 2399 Lorenz, M. C., and J. Heitman, 1998 Regulators of pseudohyphal
- 2400 differentiation in *Saccharomyces cerevisiae* identified through
- 2401 multicopy suppressor analysis in ammonium permease mutant
- 2402 strains. *Genetics* 150: 1443–1457.
- 2403 Love, M. I., W. Huber, and S. Anders, 2014 Moderated estimation
- 2404 of fold change and dispersion for RNA-seq data with DESeq2.
- 2405 *Genome Biol.* 15: 550. <https://doi.org/10.1186/s13059-014-0550-8>
- 2406 Luo, W., and C. Brouwer, 2013 Pathview: an R/Bioconductor
- 2407 package for pathway-based data integration and visualization.
- 2408 *Bioinformatics* 29: 1830–1831. <https://doi.org/10.1093/bioinformatics/btt285>
- 2409 Lyons, T. J., A. P. Gasch, L. A. Gaither, D. Botstein, P. O. Brown
- 2410 *et al.*, 2000 Genome-wide characterization of the Zap1p zinc-
- 2411 responsive regulon in yeast. *Proc. Natl. Acad. Sci. USA* 97:
- 2412 7957–7962. <https://doi.org/10.1073/pnas.97.14.7957>
- 2413 Madhani, H. D., T. Galitski, E. S. Lander, and G. R. Fink,
- 2414 1999 Effectors of a developmental mitogen-activated protein
- 2415 kinase cascade revealed by expression signatures of signaling
- 2416 mutants. *Proc. Natl. Acad. Sci. USA* 96: 12530–12535.
- 2417 <https://doi.org/10.1073/pnas.96.22.12530>
- 2418 Magasanik, B., and C. A. Kaiser, 2002 Nitrogen regulation in *Sac-*
- 2419 *charomyces cerevisiae*. *Gene* 290: 1–18. [https://doi.org/10.1016/S0378-1119\(02\)00558-9](https://doi.org/10.1016/S0378-1119(02)00558-9)
- 2420 Maricq, A. V., E. Peckol, M. Driscoll, and C. I. Bargmann,
- 2421 1995 Mechanosensory signalling in *C. elegans* mediated by
- 2422 the GLR-1 glutamate receptor. *Nature* 378: 78–81 [corrigenda:
- 2423 *Nature* 379: 749 (1996)]. <https://doi.org/10.1038/378078a0>
- 2424 Maršíková, J., D. Wilkinson, O. Hlaváček, G. D. Gilfillan, A. Mizer-
- 2425 anschi *et al.*, 2017 Metabolic differentiation of surface and in-
- 2426 vasive cells of yeast colony biofilms revealed by gene expression
- 2427 profiling. *BMC Genomics* 18: 814. <https://doi.org/10.1186/s12864-017-4214-4>
- 2428 Martnez, M. J., S. Roy, A. B. Archuletta, P. D. Wentzell, S. S. Anna-
- 2429 Arriola *et al.*, 2004 Genomic analysis of stationary-phase and

- 2427 exit in *Saccharomyces cerevisiae*: gene expression and identifica- 2483  
 2428 tion of novel essential genes. *Mol. Biol. Cell* 15: 5295–5305. 2484  
 2429 <https://doi.org/10.1091/mbc.e03-11-0856> 2485  
 2430 Miralles, V. J., and R. Serrano, 1995 A genomic locus in *Saccha-* 2486  
 2431 *romyces cerevisiae* with four genes up-regulated by osmotic 2487  
 2432 stress. *Mol. Microbiol.* 17: 653–662. [https://doi.org/10.1111/](https://doi.org/10.1111/j.1365-2958.1995.mmi_17040653.x) 2488  
 2433 [j.1365-2958.1995.mmi\\_17040653.x](https://doi.org/10.1111/j.1365-2958.1995.mmi_17040653.x) 2489  
 2434 Mösch, H. U., R. L. Roberts, and G. R. Fink, 1996 Ras2 signals via 2490  
 2435 the Cdc42/Ste20/mitogen-activated protein kinase module to 2491  
 2436 induce filamentous growth in *Saccharomyces cerevisiae*. *Proc.* 2492  
 2437 *Natl. Acad. Sci. USA* 93: 5352–5356. [https://doi.org/10.1073/](https://doi.org/10.1073/pnas.93.11.5352) 2493  
 2438 [pnas.93.11.5352](https://doi.org/10.1073/pnas.93.11.5352) 2494  
 2439 Mösch, H. U., E. Kübler, S. Krappmann, G. R. Fink, and G. H. Braus, 2495  
 2440 1999 Crosstalk between the Ras2p-controlled mitogen-acti- 2496  
 2441 vated protein kinase and cAMP pathways during invasive 2497  
 2442 growth of *Saccharomyces cerevisiae*. *Mol. Biol. Cell* 10: 1325– 2498  
 2443 1335. <https://doi.org/10.1091/mbc.10.5.1325> 2499  
 2444 Mrsa, V., M. Ecker, S. Strahl-Bolsinger, M. Nimtz, L. Lehle *et al.*, 2500  
 2445 1999 Deletion of new covalently linked cell wall glycoproteins 2501  
 2446 alters the electrophoretic mobility of phosphorylated wall com- 2502  
 2447 ponents of *Saccharomyces cerevisiae*. *J. Bacteriol.* 181: 3076–3086. 2503  
 2448 Nandi, M., C. Berry, A. K. Brassinga, M. F. Belmonte, W. G. Fernan- 2504  
 2449 dando *et al.*, 2016 *Pseudomonas brassicaearum* strain DF41 2505  
 2450 kills *Caenorhabditis elegans* through biofilm-dependent and bi- 2506  
 2451 ofilm-independent mechanisms. *Appl. Environ. Microbiol.* 82: 2507  
 2452 6889–6898. <https://doi.org/10.1128/AEM.02199-16> 2508  
 2453 Nett, J. E., and D. R. Andes, 2015 Fungal biofilms: in vivo models 2509  
 2454 for discovery of anti-biofilm drugs. *Microbiol. Spectr.* 3: 2510  
 2455 MB-0008-2014. doi: 10.1128/microbiolspec.MB-0008- 2511  
 2456 2014 <https://doi.org/10.1128/microbiolspec.MB-0008-2014> 2512  
 2457 Olson, K. A., C. Nelson, G. Tai, W. Hung, C. Yong *et al.*, 2000 2513  
 2458 Two regulators of Ste12p inhibit pheromone-responsive transcrip- 2514  
 2459 tion by separate mechanisms. *Mol. Cell. Biol.* 20: 4199–4209. 2515  
 2460 <https://doi.org/10.1128/MCB.20.12.4199-4209.2000> 2516  
 2461 Palecek, S. P., A. S. Parikh, and S. J. Kron, 2000 Genetic analysis 2517  
 2462 reveals that FLO11 upregulation and cell polarization indepen- 2518  
 2463 dently regulate invasive growth in *Saccharomyces cerevisiae*. 2519  
 2464 *Genetics* 156: 1005–1023. 2520  
 2465 Palková, Z., and L. Váchová, 2006 Life within a community: ben- 2521  
 2466 efit to yeast long-term survival. *FEMS Microbiol. Rev.* 30: 806– 2522  
 2467 824. <https://doi.org/10.1111/j.1574-6976.2006.00034.x> 2523  
 2468 Pan, X., and J. Heitman, 2000 Sok2 regulates yeast pseudohyphal 2524  
 2469 differentiation via a transcription factor cascade that regulates 2525  
 2470 cell-cell adhesion. *Mol. Cell. Biol.* 20: 8364–8372. [https://](https://doi.org/10.1128/MCB.20.22.8364-8372.2000) 2526  
 2471 [doi.org/10.1128/MCB.20.22.8364-8372.2000](https://doi.org/10.1128/MCB.20.22.8364-8372.2000) 2527  
 2472 Rabitsch, K. P., A. Toth, M. Galova, A. Schleiffer, G. Schaffner *et al.*, 2528  
 2473 2001 A screen for genes required for meiosis and spore forma- 2529  
 2474 tion based on whole-genome expression. *Curr. Biol.* 11: 1001– 2530  
 2475 1009. [https://doi.org/10.1016/S0960-9822\(01\)00274-3](https://doi.org/10.1016/S0960-9822(01)00274-3) 2531  
 2476 Ramage, G., S. P. Saville, D. P. Thomas, and J. L. Lopez-Ribot, 2532  
 2477 2005 *Candida* biofilms: an update. *Eukaryot. Cell* 4: 633– 2533  
 2478 638. <https://doi.org/10.1128/EC.4.4.633-638.2005> 2534  
 2479 Reiner, A., D. Yekutieli, and Y. Benjamini, 2003 Identifying differ- 2535  
 2480 entially expressed genes using false discovery rate controlling 2536  
 2481 procedures. *Bioinformatics* 19: 368–375. [https://doi.org/](https://doi.org/10.1093/bioinformatics/btf877) 2537  
 2482 [10.1093/bioinformatics/btf877](https://doi.org/10.1093/bioinformatics/btf877) 2538  
 2483 Reynolds, T. B., 2006 The Opi1p transcription factor affects ex- 2539  
 2484 pression of FLO11, mat formation, and invasive growth in *Sac-* 2540  
 2485 *charomyces cerevisiae*. *Eukaryot. Cell* 5: 1266–1275. [https://](https://doi.org/10.1128/EC.00022-06) 2541  
 2486 [doi.org/10.1128/EC.00022-06](https://doi.org/10.1128/EC.00022-06) 2542  
 2487 Reynolds, T. B., and G. R. Fink, 2001 Bakers' yeast, a model for 2543  
 2488 fungal biofilm formation. *Science* 291: 878–881. [https://](https://doi.org/10.1126/science.291.5505.878) 2544  
 2489 [doi.org/10.1126/science.291.5505.878](https://doi.org/10.1126/science.291.5505.878) 2545  
 2490 Roberts, C. J., B. Nelson, M. J. Marton, R. Stoughton, M. R. Meyer 2546  
 2491 *et al.*, 2000 Signaling and circuitry of multiple MAPK pathways 2547  
 2492 revealed by a matrix of global gene expression profiles. *Science* 2548  
 2493 287: 873–880. <https://doi.org/10.1126/science.287.5454.873> 2549  
 2494 Roberts, R. L., and G. R. Fink, 1994 Elements of a single MAP 2550  
 2495 kinase cascade in *Saccharomyces cerevisiae* mediate two devel- 2551  
 2496 opmental programs in the same cell type: mating and invasive 2552  
 2497 growth. *Genes Dev.* 8: 2974–2985. [https://doi.org/10.1101/](https://doi.org/10.1101/gad.8.24.2974) 2553  
 2498 [gad.8.24.2974](https://doi.org/10.1101/gad.8.24.2974) 2554  
 2499 Robertson, L. S., and G. R. Fink, 1998 The three yeast A kinases 2555  
 2500 have specific signaling functions in pseudohyphal growth. *Proc.* 2556  
 2501 *Natl. Acad. Sci. USA* 95: 13783–13787. [https://doi.org/](https://doi.org/10.1073/pnas.95.23.13783) 2557  
 2502 [10.1073/pnas.95.23.13783](https://doi.org/10.1073/pnas.95.23.13783) 2558  
 2503 Robinson, M. D., D. J. McCarthy, and G. K. Smyth, 2010 edgeR: a 2559  
 2504 Bioconductor package for differential expression analysis of dig- 2560  
 2505 ital gene expression data. *Bioinformatics* 26: 139–140. [https://](https://doi.org/10.1093/bioinformatics/btp616) 2561  
 2506 [doi.org/10.1093/bioinformatics/btp616](https://doi.org/10.1093/bioinformatics/btp616) 2562  
 2507 Rodríguez-Porrata, B., D. Carmona-Gutierrez, A. Reisenbichler, M. 2563  
 2508 Bauer, G. Lopez *et al.*, 2012 Sip18 hydrophilin prevents yeast 2564  
 2509 cell death during desiccation stress. *J. Appl. Microbiol.* 112: 2565  
 2510 512–525. <https://doi.org/10.1111/j.1365-2672.2011.05219.x> 2566  
 2511 Rose, M. D., F. Winston, and P. Heieter, 1990 *Methods in Yeast* 2567  
 2512 *Genetics*. Cold Spring Harbor Laboratory Press, Cold Spring Har- 2568  
 2513 bor, NY. 2569  
 2514 Rupp, S., E. Summers, H. J. Lo, H. Madhani, and G. Fink, 2570  
 2515 1999 MAP kinase and cAMP filamentation signaling pathways 2571  
 2516 converge on the unusually large promoter of the yeast FLO11 2572  
 2517 gene. *EMBO J.* 18: 1257–1269. [https://doi.org/10.1093/em-](https://doi.org/10.1093/emboj/18.5.1257) 2573  
 2518 [boj/18.5.1257](https://doi.org/10.1093/emboj/18.5.1257) 2574  
 2519 Ryan, O., R. S. Shapiro, C. F. Kurat, D. Mayhew, A. Baryshnikova 2575  
 2520 *et al.*, 2012 Global gene deletion analysis exploring yeast fila- 2576  
 2521 mentous growth. *Science* 337: 1353–1356. [https://doi.org/](https://doi.org/10.1126/science.1224339) 2577  
 2522 [10.1126/science.1224339](https://doi.org/10.1126/science.1224339) 2578  
 2523 Samanta, M. P., and S. Liang, 2003 Predicting protein functions 2579  
 2524 from redundancies in large-scale protein interaction networks. 2580  
 2525 *Proc. Natl. Acad. Sci. USA* 100: 12579–12583. [https://doi.org/](https://doi.org/10.1073/pnas.2132527100) 2581  
 2526 [10.1073/pnas.2132527100](https://doi.org/10.1073/pnas.2132527100) 2582  
 2527 Sambrook, J., E. F. Fritsch, and T. Maniatis, 1989 *Molecular Clon-* 2583  
 2528 *ing: A Laboratory Manual*. Cold Spring Harbor Laboratory Press, 2584  
 2529 Cold Spring Harbor, NY. 2585  
 2530 Sarkar, P. K., M. A. Florczyk, K. A. McDonough, and D. K. Nag, 2586  
 2531 2002 SSP2, a sporulation-specific gene necessary for outer 2587  
 2532 spore wall assembly in the yeast *Saccharomyces cerevisiae*. 2588  
 2533 *Mol. Genet. Genomics* 267: 348–358. [https://doi.org/](https://doi.org/10.1007/s00438-002-0666-5) 2589  
 2534 [10.1007/s00438-002-0666-5](https://doi.org/10.1007/s00438-002-0666-5) 2590  
 2535 Sarode, N., B. Miracle, X. Peng, O. Ryan, and T. B. Reynolds, 2591  
 2536 2011 Vacuolar protein sorting genes regulate mat formation 2592  
 2537 in *Saccharomyces cerevisiae* by Flo11p-dependent and -inde- 2593  
 2538 pendent mechanisms. *Eukaryot. Cell* 10: 1516–1526. [https://](https://doi.org/10.1128/EC.05078-11) 2594  
 2539 [doi.org/10.1128/EC.05078-11](https://doi.org/10.1128/EC.05078-11) 2595  
 2540 Sarode, N., S. E. Davis, R. N. Tams, and T. B. Reynolds, 2014 The 2596  
 2541 Wsc1p cell wall signaling protein controls biofilm (Mat) forma- 2597  
 2542 tion independently of Flo11p in *Saccharomyces cerevisiae*. *G3* 2598  
 2543 (Bethesda) 4: 199–207. <https://doi.org/10.1534/g3.113.006361> 2599  
 2544 Scherz, K., R. Andersen, L. Bojsen, Gro, Rejtkjær *et al.*, 2600  
 2545 2014 Genetic basis for *Saccharomyces cerevisiae* biofilm in 2601  
 2546 liquid medium. *G3* (Bethesda) 4: 1671–1680. [https://doi.org/](https://doi.org/10.1534/g3.114.010892) 2602  
 2547 [10.1534/g3.114.010892](https://doi.org/10.1534/g3.114.010892) 2603  
 2548 Schmalix, W., and W. Bandlow, 1993 The ethanol-inducible YAT1 2604  
 2549 gene from yeast encodes a presumptive mitochondrial outer 2605  
 2550 carnitine acetyltransferase. *J. Biol. Chem.* 268: 27428–27439. 2606  
 2551 Sertill, O., B. D. Cohen, K. J. Davies, and C. V. Lowry, 1997 The 2607  
 2552 DAN1 gene of *S. cerevisiae* is regulated in parallel with the 2608  
 2553 hypoxic genes, but by a different mechanism. *Gene* 192: 199– 2609  
 2554 205. [https://doi.org/10.1016/S0378-1119\(97\)00028-0](https://doi.org/10.1016/S0378-1119(97)00028-0) 2610  
 2555 Shtonda, B. B., and L. Avery, 2006 Dietary choice behavior in 2611  
 2556 *Caenorhabditis elegans*. *J. Exp. Biol.* 209: 89–102. [https://](https://doi.org/10.1242/jeb.01955) 2612  
 2557 [doi.org/10.1242/jeb.01955](https://doi.org/10.1242/jeb.01955) 2613  
 2558 Small, W. C., R. D. Brodeur, A. Sandor, N. Fedorova, G. Li *et al.*, 2614  
 2559 1995 Enzymatic and metabolic studies on retrograde regula- 2615  
 2560 tion. *J. Biol. Chem.* 270: 11111–11116. <https://doi.org/10.1074/jbc.270.23.11111> 2616

- 2539 tion mutants of yeast. *Biochemistry* 34: 5569–5576. <https://doi.org/10.1021/bi00016a031>
- 2540 Smukalla, S., M. Caldara, N. Pochet, A. Beauvais, S. Guadagnini
- 2541 *et al.*, 2008 FLO1 is a variable green beard gene that drives
- 2542 biofilm-like cooperation in budding yeast. *Cell* 135: 726–737.
- 2543 <https://doi.org/10.1016/j.cell.2008.09.037>
- 2544 Soll, D. R., and K. J. Daniels, 2016 Plasticity of *Candida albicans*
- 2545 biofilms. *Microbiol. Mol. Biol. Rev.* 80: 565–595. <https://doi.org/10.1128/MMBR.00068-15>
- 2546 Stefan, C. J., S. M. Padilla, A. Audhya, and S. D. Emr, 2005 The
- 2547 phosphoinositide phosphatase Sjl2 is recruited to cortical actin
- 2548 patches in the control of vesicle formation and fission during
- 2549 endocytosis. *Mol. Cell. Biol.* 25: 2910–2923. <https://doi.org/10.1128/MCB.25.8.2910-2923.2005>
- 2550 Stefanini, I., L. Dapporto, L. Berna, M. Polsinelli, S. Turillazzi *et al.*,
- 2551 2016 Social wasps are a *Saccharomyces* mating nest. *Proc.*
- 2552 *Natl. Acad. Sci. USA* 113: 2247–2251. <https://doi.org/10.1073/pnas.1516453113>
- 2553 Sterner, D. E., and S. L. Berger, 2000 Acetylation of histones and
- 2554 transcription-related factors. *Microbiol. Mol. Biol. Rev.* 64: 435–
- 2555 459. <https://doi.org/10.1128/MMBR.64.2.435-459.2000>
- 2556 Sudbery, P., N. Gow, and J. Berman, 2004 The distinct morpho-
- 2557 genic states of *Candida albicans*. *Trends Microbiol.* 12: 317–
- 2558 324. <https://doi.org/10.1016/j.tim.2004.05.008>
- 2559 Suissa, M., K. Suda, and G. Schatz, 1984 Isolation of the nuclear
- 2560 yeast genes for citrate synthase and fifteen other mitochondrial
- 2561 proteins by a new screening method. *EMBO J.* 3: 1773–1781.
- 2562 <https://doi.org/10.1002/j.1460-2075.1984.tb02045.x>
- 2563 Swiegers, J. H., N. Dippenaar, I. S. Pretorius, and F. F. Bauer,
- 2564 2001 Carnitine-dependent metabolic activities in *Saccharomyces cerevisiae*: three carnitine acetyltransferases are essential in a carnitine-dependent strain. *Yeast* 18: 585–595. <https://doi.org/10.1002/yea.712>
- 2565 Swiegers, J. H., I. S. Pretorius, and F. F. Bauer, 2006 Regulation of
- 2566 respiratory growth by Ras: the glyoxylate cycle mutant, cit2-
- 2567 Delta, is suppressed by RAS2. *Curr. Genet.* 50: 161–171.
- 2568 <https://doi.org/10.1007/s00294-006-0084-z>
- 2569 Tam, A., J. E. F. Green, S. Balasuriya, E. L. Tek, J. M. Gardner *et al.*,
- 2570 2018 Nutrient-limited growth with non-linear cell diffusion as
- 2571 a mechanism for floral pattern formation in yeast biofilms.
- 2572 *J. Theor. Biol.* 448: 122–141. <https://doi.org/10.1016/j.jtbi.2018.04.004>
- 2573 Tedford, K., S. Kim, D. Sa, K. Stevens, and M. Tyers,
- 2574 1997 Regulation of the mating pheromone and invasive
- 2575 growth responses in yeast by two MAP kinase substrates. *Curr. Biol.*
- 2576 7: 228–238. [https://doi.org/10.1016/S0960-9822\(06\)00118-7](https://doi.org/10.1016/S0960-9822(06)00118-7)
- 2577 Trapnell, C., L. Pachter, and S. L. Salzberg, 2009 TopHat: discover-
- 2578 ing splice junctions with RNA-Seq. *Bioinformatics* 25: 1105–
- 2579 1111. <https://doi.org/10.1093/bioinformatics/btp120>
- 2580 Traven, A., A. Janicke, P. Harrison, A. Swaminathan, T. Seemann
- 2581 *et al.*, 2012 Transcriptional profiling of a yeast colony provides
- 2582 new insight into the heterogeneity of multicellular fungal com-
- 2583 munities. *PLoS One* 7: e46243. <https://doi.org/10.1371/journal.pone.0046243>
- 2584 Váchová, L., V. Stovicek, O. Hlaváček, O. Chernyavskiy, L. Stěpánek
- 2585 *et al.*, 2011 Flo11p, drug efflux pumps, and the extracellular
- 2586 matrix cooperate to form biofilm yeast colonies. *J. Cell Biol.*
- 2587 194: 679–687. <https://doi.org/10.1083/jcb.201103129>
- 2588 Vaitkevicius, K., B. Lindmark, G. Ou, T. Song, C. Toma *et al.*,
- 2589 2006 A *Vibrio cholerae* protease needed for killing of *Caenorhabditis elegans* has a role in protection from natural predator grazing. *Proc. Natl. Acad. Sci. USA* 103: 9280–9285. <https://doi.org/10.1073/pnas.0601754103>
- 2590 van der Felden, J., S. Weisser, S. Bruckner, P. Lenz, and H. U.
- 2591 Mosch, 2014 The transcription factors Tec1 and Ste12 interact with coregulators Msa1 and Msa2 to activate adhesion and multicellular development. *Mol. Cell. Biol.* 34: 2283–2293. <https://doi.org/10.1128/MCB.01599-13>
- van Dyk, D., I. S. Pretorius, and F. F. Bauer, 2005 Mss11p is a central element of the regulatory network that controls FLO11 expression and invasive growth in *Saccharomyces cerevisiae*. *Genetics* 169: 91–106. <https://doi.org/10.1534/genetics.104.033704>
- Voordeckers, K., D. De Maeyer, E. van der Zande, M. D. Vinces, W. Meert *et al.*, 2012 Identification of a complex genetic network underlying *Saccharomyces cerevisiae* colony morphology. *Mol. Microbiol.* 86: 225–239. <https://doi.org/10.1111/j.1365-2958.2012.08192.x>
- Wang, L., and S. Y. Dent, 2014 Functions of SAGA in development and disease. *Epigenomics* 6: 329–339. <https://doi.org/10.2217/epi.14.22>
- West, S. A., A. S. Griffin, and A. Gardner, 2007 Evolutionary explanations for cooperation. *Curr. Biol.* 17: R661–R672. <https://doi.org/10.1016/j.cub.2007.06.004>
- Wickham, H., 2016 *ggplot2: Elegant Graphics for Data Analysis*. Springer-Verlag, New York.
- Wilson, M. A., C. V. St Amour, J. L. Collins, D. Ringe, and G. A. Petsko, 2004 The 1.8-Å resolution crystal structure of YDR533Cp from *Saccharomyces cerevisiae*: a member of the DJ-1/ThiJ/PfpI superfamily. *Proc. Natl. Acad. Sci. USA* 101: 1531–1536. <https://doi.org/10.1073/pnas.0308089100>
- Winston, F., C. Dollard, E. A. Malone, J. Clare, J. G. Kapakos *et al.*, 1987 Three genes are required for trans-activation of Ty transcription in yeast. *Genetics* 115: 649–656.
- Wood, W. B., 1988 *The Nematode Caenorhabditis elegans*. Cold Spring Harbor Laboratory Press, Cold Spring Harbor, New York.
- Wu, C. Y., A. J. Bird, L. M. Chung, M. A. Newton, D. R. Winge *et al.*,
- 2008 Differential control of Zap1-regulated genes in response to zinc deficiency in *Saccharomyces cerevisiae*. *BMC Genomics* 9: 370. <https://doi.org/10.1186/1471-2164-9-370>
- Xu, T., C. A. Shively, R. Jin, M. J. Eckwahl, C. J. Dobry *et al.*,
- 2010 A profile of differentially abundant proteins at the yeast cell periphery during pseudohyphal growth. *J. Biol. Chem.* 285: 15476–15488. <https://doi.org/10.1074/jbc.M110.114926>
- Yuan, D. S., 2000 Zinc-regulated genes in *Saccharomyces cerevisiae* revealed by transposon tagging. *Genetics* 156: 45–58.
- Zaman, S., S. I. Lippman, X. Zhao, and J. R. Broach, 2008 How *Saccharomyces* responds to nutrients. *Annu. Rev. Genet.* 42: 27–81. <https://doi.org/10.1146/annurev.genet.41.110306.130206>
- Zara, G., M. Budroni, I. Mannazzu, and S. Zara, 2011 Air-liquid biofilm formation is dependent on ammonium depletion in a *Saccharomyces cerevisiae* flor strain. *Yeast* 28: 809–814. <https://doi.org/10.1002/yea.1907>
- Zeitlinger, J., I. Simon, C. T. Harbison, N. M. Hannett, T. L. Volkert *et al.*, 2003 Program-specific distribution of a transcription factor dependent on partner transcription factor and MAPK signaling. *Cell* 113: 395–404. [https://doi.org/10.1016/S0092-8674\(03\)00301-5](https://doi.org/10.1016/S0092-8674(03)00301-5)
- Zhao, H., and D. Eide, 1996 The yeast ZRT1 gene encodes the zinc transporter protein of a high-affinity uptake system induced by zinc limitation. *Proc. Natl. Acad. Sci. USA* 93: 2454–2458. <https://doi.org/10.1073/pnas.93.6.2454>
- Zhao, H., and D. J. Eide, 1997 Zap1p, a metalloregulatory protein involved in zinc-responsive transcriptional regulation in *Saccharomyces cerevisiae*. *Mol. Cell. Biol.* 17: 5044–5052. <https://doi.org/10.1128/MCB.17.9.5044>
- Zhu, A., J. G. Ibrahim, and M. I. Love, 2018 Heavy-tailed prior distributions for sequence count data: removing the noise and preserving large differences. *Bioinformatics*. DOI: 10.1093/bioinformatics/bty895. <https://doi.org/10.1093/bioinformatics/bty895>

Communicating editor: M. Freitag



**Genetics July (2019)**  
**Author query sheet Chow (GEN\_302004)**

Do you want to participate in the Author's Choice Open Access option for your article?

- No  
 Yes, Standard Open Access  
 Yes, Creative Commons CC BY 4.0 License

Both Author Choice Open options make your article freely available to all readers (regardless of subscription) immediately after publication. With the Standard Author Choice Open Access, copyright remains with the Genetics Society of America as outlined in our copyright policy and future re-use of your content by others requires permission from GSA. With the CC BY 4.0 option, you hold copyright on the article, but anyone can share or adapt for any purpose, even commercially so long as they attribute the original source. Some authors have explained that they do not wish to grant others the right to modify and/or sell their content, so we offer both choices for the content to be made freely-available. Both Open Access options carry a surcharge of \$1500 for GSA members or \$2000 for non-members

More information: <http://www.genetics.org/content/after-acceptance#charges>

**QA1** If you or your coauthors would like to include an ORCID ID in this article, please provide your respective ORCID IDs along with your corrections.

Note: If you do not yet have an ORCID ID and would like one, you may register for this unique digital identifier at <https://orcid.org/register>.



- 1 Please verify corresponding author address.
- 2 Please check all figure legends carefully to confirm that any and all labels, designators, directionals, colors, etc. are represented accurately in comparison with the figure images.
- 3 Any alternations between capitalization and/or italics in genetic and taxonomic nomenclature have been retained per the original manuscript. *Genetics* style is for genes and alleles to be italicized; please confirm that all nomenclature has been formatted properly throughout. Per journal style, uppercase Greek letters should remain roman even when appearing in a term where the overall style is italic (e.g., a gene name such as *kap108Δ*). Note that headings are set all roman or all italics based on journal style and should not be changed.
- 4 Please confirm or update any and all URLs in your article.
- 5 Please check the Saccharomyces Genome Database links throughout. A list of entities linked in this article is available at [http://textpresso-dev.caltech.edu/gsa/yeast/entity\\_link\\_tables/302004.html](http://textpresso-dev.caltech.edu/gsa/yeast/entity_link_tables/302004.html).
- 6 If an abbreviation, please spell out "IHW" at first mention.
- 7 Please provide all author initials and surnames for "Chow *et al.*, personal communication."
- 8 Please provide all author initials and surnames for "Chow *et al.*, unpublished data," and update the information if it has been accepted for publication.
- 9 Please provide all author initials and surnames for "Prabhakar *et al.*, personal communication."
- 10 If abbreviations, please spell out "ASH," "FLP," and "OLQ" at first mention.
- 11 Please check and confirm whether "the standard difference between experiments" means "the SD between experiments."

